

## REMARKS

Applicant respectfully requests reconsideration of the present application in view of the foregoing amendments and in view of the reasons that follow.

### A. Claim Amendments.

Claim 18 is amended and new claims 36-38 are added. Claims 20-23 and 32-35 were previously cancelled. Claims 25-31 were previously withdrawn. After amendment, claims 18, 19, 24, and 36-38 will remain pending and under consideration.

The claims have been amended to recite that delivery of the expression construct is to cardiomyocytes. Support for the amendment and new claims may be found throughout the specification, *e.g.*, paragraphs 0018 and 0061, and in the claims as filed. No new matter is added by this amendment, entry of which is therefore requested.

### B. Response to Rejection under 35 USC Section 112, First Paragraph (enablement)

Claims 18, 19, and 24 remain rejected for lack of enablement. Applicants respectfully traverse the rejection as it may apply to the amended claims for the reasons already of record and those that follow.

The Action alleges, as a first issue, that S16E PLB gene therapy is an unpredictable art with respect to targeting any and all myocytes *in vivo* by any and all routes of administration of the S16E PLB expression construct. Without acquiescing in the substantive basis of the rejection, Applicants have amended the claims to recite that the phospholamban gene encoding protein having an S16E mutation is administered to cardiomyocytes. Thus, the S16E PLB expression construct is not administered “to any and all myocytes.” Rather, the S16E PLB

expression construct is administered to cardiomyocytes, where expression of the encoded protein can mediate improved cardiac muscle contractility.

Moreover, Applicants respectfully submit that the Examiner's concern that the claims encompass administration "by any and all routes of administration," has been rendered moot by the amendment to claim 18. Specifically, claim 18 has been amended to require that the expression construct be delivered to cardiomyocytes. It is respectfully submitted that the skilled artisan would recognize that not any and all routes of administration would be suitable for achieving administration to cardiomyocytes. Indeed, the reference cited by the Examiner (Thompson *et al.*, *Annals of Med* 36(Suppl 1):106-15, 2004) and the primary references therein establish that effective methods of delivery of genes to cardiomyocytes were well-known in the art at the time of filing. For similar reasons, Applicants submit that this rejection does not apply to newly added claim 36, and claims 37-38 depending therefrom, which recites that the expression construct is administered to cardiomyocytes via intracoronary administration.

The Examiner further asserts that "the transient nature of transgene expression with adenoviral vectors may limit the use of these vectors to the treatment of acute vascular injury and have less utility in treating chronic or progressive disorders such as heart failure and atherosclerosis," citing Barbato *et al.* (*Critical Reviews in Clin Lab Sci* 40(5):499-545, 2003) (Office Action at page 4). Contrary to the Examiner's assertion, Applicants have demonstrated sustained expression of the S16E PLB transgene in a hamster model of cardiomyopathy (see Applicants' co-pending application Serial No. 09/954,571 (US PG Pub. No. 2002/0032167, filed 9/11/2001). Specifically, Applicants provide at paragraph 0040 of the '571 application that,

This effect of AAV-S16EPLB to mitigate the development of heart failure was further evident at 3-6 months post-gene transfer, with a substantial improvement in % FS ... and mVcf .... The high fidelity left ventricular pressure measurement directly documented that the AAV mediated delivery of the pseudophosphorylation mutant PLB sustained its rescue

effect on cardiac contractility for at 3 months post-gene delivery ... displaying an over 50% increase of LV max dP/dt in the S16EPLB-transferred animals compared to LacZ controls.

Moreover, the presence of the S16E PLB gene and its protein product over this time period were confirmed by Southern blotting and immunoblotting. Thus, these data provide concrete evidence of sustained expression of S16E PLB using the AAV vector and support the operability of the present methods.

As to the adenoviral vector whose use is discussed by Barbato, *et al.*, it will be appreciated that even transient changes in contractile function in the heart can be beneficial; e.g., in acute therapy pending surgical intervention, such as transplantation (see, e.g., Giordano, *et al.*, *Nat. Med.*, 2:534-539, 1996).

The Action further alleges, as a second issue, that because of the complexities involved in the etiology of loss of cardiac muscle contractility associated with heart failure, the specification allegedly fails to establish the S16E mutant PLB gene is capable of treating loss of cardiac muscle contractility associated with heart failure. To the contrary, however, post-filing data confirms the operability of the present methods in treating heart failure *regardless* of the underlying cause of that heart failure. Specifically, the inventors have confirmed the operability of the claimed methods in a number of different heart failure models in different animal species.

For example, in the study discussed above, the inventors demonstrated the ability of the S16E PLB transgene to mitigate the development of heart failure in the cardiomyopathic hamster model of progressive heart failure, a model of a human genetic disease. In particular, the inventors demonstrated that the S16E PLB transgene provided a sustained rescue effect on cardiac contractility and improved a number of measures of cardiac function.

In another study, the inventors studied the effects of the S16E PLB transgene in rats with heart failure after myocardial infarction (MI), a model of acquired disease. Specifically, the inventors showed that “in vivo delivery of the S16EPLN gene was highly effective in improving LV function and mitigating adverse remodeling compared with delivery of saline” (see Iwanaga *et al.*, *J Clin Investigation* 113(5):727-36, 2004 at p. 732, col. 2; copy attached). The results reported provide concrete evidence that treatment of MI rats with S16E PLB improved contractility in addition to other cardiac function parameters and that such improvement was sustained over the 6-month observation period. The inventors conclude that these finding document that the therapeutic effects of the present methods can be extended to acquired forms of heart failure.

In yet another study, S16E PLB gene therapy in sheep with moderate-to-severe pacing-induced heart failure was shown to enhance cardiac contractility in heart failure (*see* Hoshijima *et al.*, *J Amer Coll Cardiology* 48(9 Suppl A):A15-A23, 2006 at p. A21, col. 2; copy attached). Taken together these studies establish that the claimed methods are effective in treating heart failure regardless of the particular etiology (*e.g.*, genetic or acquired) of heart failure in each model.

In summary, the evidence of record therefore confirms what the Specification asserts: the S16E phospholamban molecule, delivered to the heart in an expression construct, improves cardiac contractility. Specifically, practice of the invention to treat heart failure by improving cardiac contractility has been demonstrated in several art-accepted models of heart failure. Therefore, it is respectfully submitted that based on the Specification and the post-filing data, the skilled artisan would reasonably expect success in using the claimed methods to improve cardiac contractility in the failing heart without the need for undue experimentation.

Applicant respectfully submits that the foregoing establishes that the Specification enables use of the invention to suppress phospholamban activity in the heart, allowing SERCA2 mediated contractility to improve to treat heart failure, the target condition recited in all pending claims (see Claim 18). Accordingly, reconsideration and withdrawal of the enablement rejection under 35 U.S.C. §112, first paragraph are therefore respectfully requested.

**C. Rejection under Nonstatutory Obviousness-Type Double Patenting**

The provisional rejection of claims 18, 19, and 24 on the ground of nonstatutory obviousness-type double patenting as allegedly unpatentable over claims 70-72 and 98-101 of co-pending Application No. 09/954,571 (hereinafter “the ‘571 application”) is respectfully traversed.

While not acquiescing to the substantive basis for this rejection, in order to reduce the issues and expedite prosecution, a terminal disclaimer over a patent that may issue from the commonly-owned ‘571 application is submitted herewith. Accordingly, reconsideration and withdrawal of this rejection are respectfully requested.

In re Application of:  
Chien et al.  
Application No.: 10/705,791  
Filed: November 10, 2003  
Page 10

PATENT  
Attorney Docket No.: ST-UCSD3230-1

### CONCLUSION


Applicant believes that the present application is now in condition for allowance.  
Favorable reconsideration of the application as amended is respectfully requested.

The Examiner is invited to contact the undersigned by telephone if it is felt that a telephone interview would advance the prosecution of the present application.

No fee is believed due in connection with this Amendment. If any additional fees are due, the Commissioner is hereby authorized to charge any fees that may be required by this paper to Deposit Account No. 07-1896 referencing the above-identified attorney docket number.

Respectfully submitted,

Date: February 28, 2008

  
Stacy L. Taylor  
Registration No. 34,842  
Telephone: (858) 677-1423  
Facsimile: (858) 677-1465

DLA PIPER US LLP  
4365 Executive Drive, Suite 1100  
San Diego, California 92121-2133  
**USPTO Customer Number 28213**

Attachments: Iwanaga et al., J Clin Investigation 113(5):727-36, 2004  
Hoshijima et al., J Amer Coll Cardiology 48(9 Suppl A):A15-A23, 2006

# Chronic phospholamban inhibition prevents progressive cardiac dysfunction and pathological remodeling after infarction in rats

Yoshitaka Iwanaga,<sup>1,2</sup> Masahiko Hoshijima,<sup>1,2</sup> Yusu Gu,<sup>1,2</sup> Mitsuo Iwatate,<sup>1,2</sup> Thomas Dieterle,<sup>1,2</sup> Yasuhiko Ikeda,<sup>1,2,3</sup> Moto-o Date,<sup>1,2</sup> Jacqueline Chrast,<sup>1,2</sup> Masunori Matsuzaki,<sup>3</sup> Kirk L. Peterson,<sup>1,2</sup> Kenneth R. Chien,<sup>1,2</sup> and John Ross, Jr.<sup>1,2</sup>

<sup>1</sup>Department of Medicine, and <sup>2</sup>Institute of Molecular Medicine, University of California, San Diego, La Jolla, California, USA. <sup>3</sup>Department of Medical Bioregulation, Yamaguchi University Graduate School of Medicine, Yamaguchi, Japan.

**Ablation or inhibition of phospholamban (PLN) has favorable effects in several genetic murine dilated cardiomyopathies, and we showed previously that a pseudophosphorylated form of PLN mutant (S16EPLN) successfully prevented progressive heart failure in cardiomyopathic hamsters. In this study, the effects of PLN inhibition were examined in rats with heart failure after myocardial infarction (MI), a model of acquired disease. S16EPLN was delivered into failing hearts 5 weeks after MI by transcoronary gene transfer using a recombinant adeno-associated virus (rAAV) vector. In treated (MI-S16EPLN,  $n = 16$ ) and control (MI-saline,  $n = 18$ ) groups, infarct sizes were closely matched and the left ventricle was similarly depressed and dilated before gene transfer. At 2 and 6 months after gene transfer, MI-S16EPLN rats showed an increase in left ventricular (LV) ejection fraction and a much smaller rise in LV end-diastolic volume, compared with progressive deterioration of LV size and function in MI-saline rats. Hemodynamic measurements at 6 months showed lower LV end-diastolic pressures, with enhanced LV function (contractility and relaxation), lowered LV mass and myocyte size, and less fibrosis in MI-S16EPLN rats. Thus, PLN inhibition by in vivo rAAV gene transfer is an effective strategy for the chronic treatment of an acquired form of established heart failure.**

## Introduction

Advances in medical and surgical treatments have substantially reduced the mortality from cardiac disease, but chronic heart failure primarily of ischemic origin remains a leading cause of morbidity and mortality (1). Given the limits of cardiac transplantation (2), new forms of treatment are needed that can target the underlying biological processes within the cardiomyocyte that lead to chronic dysfunction and unfavorable remodeling (3, 4). Gene therapy has been proposed as one such promising strategy. However, there have been several limitations to the application of gene transfer for clinical and experimental heart failure, including lack of a gene-delivery system that can provide high efficiency and cardiac specificity, and the need for vectors that give stable long-term expression (5). Recently, we developed a novel in vivo transcoronary gene-delivery system that achieved high efficiency in myocardium when applied in the cardiomyopathic hamster using an adenovirus vector (6), and relatively cardiac-specific, long-term expression was then achieved with a recombinant adeno-associated virus (rAAV) vector in that hamster model (7).

Failing heart muscle generally exhibits distinct changes in intracellular  $\text{Ca}^{2+}$  handling, including impaired removal of cytosolic  $\text{Ca}^{2+}$ ;

reduced  $\text{Ca}^{2+}$  loading of the cardiac sarcoplasmic reticulum (SR) with downregulation of SR  $\text{Ca}^{2+}$ -ATPase 2 (SERCA2); and defects in SR  $\text{Ca}^{2+}$  release accompanied by impairment of cardiac relaxation and systolic function (8, 9). However, therapeutic attempts to target these molecular abnormalities for the treatment of experimental heart failure using in vivo gene transfer strategies were limited to short-term overexpression of SERCA2 (10) or overexpression of upstream regulators of  $\text{Ca}^{2+}$  handling, such as a  $\beta$ -adrenergic receptor kinase-inhibitory peptide (11) using adenovirus vectors.

Initially, we crossed mice with ablated phospholamban (PLN), an endogenous inhibitor of SERCA2, with a muscle-specific Lim protein-null (MLP-null) mouse model of dilated cardiomyopathy and demonstrated complete prevention of the heart failure phenotype in the offspring, along with improved cardiac SR  $\text{Ca}^{2+}$  storage and release (12). Subsequently a PLN-null mutation was reported to prevent systolic dysfunction and exercise intolerance, but not hypertrophy, in a murine model of hypertrophic cardiomyopathy (13). Later, we generated a pseudophosphorylated mutant PLN peptide, S16EPLN, designed to mimic the conformational changes in PLN following its phosphorylation by cAMP-dependent protein kinase, and when the S16EPLN gene was delivered into BIO14.6 cardiomyopathic hamsters, the usually rapid progression of cardiac dysfunction over the 7-month study period was substantially alleviated (7).

Recent studies in transgenic models, however, have not supported a therapeutic effect of PLN ablation on cardiac hypertrophy and dysfunction. In one study, apoptotic heart failure resulted from overexpression of a signaling molecule, or severe neonatal-onset cardiac dilation was induced by targeted mutation of a structural protein, and neither was modified by PLN ablation (14). Also, Kiriazis et al. have reported that hyperdynamic PLN-null mice do not differ

**Nonstandard abbreviations used:** calcium/calmodulin-dependent kinase II (CaMKII), early mitral orifice inflow velocity (E), inflow velocity during atrial contraction (A), left ventricular (LV), LV ejection fraction (LVEF), LV end-diastolic pressure (LVEDP), LV end-diastolic volume (LVEDV), LV end-systolic volume (LVESV), muscle-specific Lim protein (MLP), myocardial infarction (MI), phospholamban (PLN), recombinant adeno-associated virus (rAAV), sarcoplasmic reticulum (SR), SR  $\text{Ca}^{2+}$ -ATPase 2 (SERCA2).

**Conflict of interest:** Kenneth Chien and Masahiko Hoshijima have a financial interest in these studies.

**Citation for this article:** *J. Clin. Invest.* 113:727–736 (2004). doi:10.1172/JCI200418716.

from wild-type mice in the development of hypertrophy or in the incidence of heart failure after sustained surgical aortic stenosis (15).

In addition, two recent clinical studies have suggested the possibility that interference with the PLN-SERCA2 interaction may be detrimental. Two types of human PLN mutations (R9C and L39stop) were linked to human dilated cardiomyopathy, and distinctive mechanisms were proposed for each mutation to induce cardiac defects by altering SR  $\text{Ca}^{2+}$  handling (16, 17).

Thus, it is critical to evaluate the role of PLN inhibition in a model of acquired heart failure that has proven fidelity and predictability for therapeutic effects in human disease. The progressive heart failure that occurs after myocardial infarction (MI) in the rat is a validated and widely accepted model of the most common form of heart failure observed in humans. In the present study, we successfully applied a modified transcatheter gene-delivery method in chronically failing hearts of rats after MI. The goal of the study was to determine whether sustained action of the S16EPLN protein in this model could affect global left ventricular (LV) function and remodeling in the setting of established heart failure.

## Methods

Experiments were carried out in adult male Sprague-Dawley rats obtained from Charles River Laboratories Inc. (Wilmington, Massachusetts, USA). The animals were housed at  $20^{\circ}\text{C} \pm 2^{\circ}\text{C}$ , 55%  $\pm$  20% humidity, with 12-hour light/dark cycles and free access to food and water in the Animal Care Facility at the University of California, San Diego. The study was approved by the University of California, San Diego Animal Subjects Committee.

**Construction of recombinant viral vectors.** rAAV vectors carrying S16EPLN (rAAV-S16EPLN) and rAAV vectors carrying a LacZ marker gene (rAAV-LacZ) were constructed as previously described (7) and produced by Lili Wang and James Wilson at the University of Pennsylvania (Philadelphia, Pennsylvania, USA). In brief, rAAV type 2 vectors were made by the three-plasmid cotransfection method (18) and recovered by a single-step heparin-column method (19). The genome titer (genome copy) was determined by real-time PCR. Recombinant adenovirus type 5 vectors with the LacZ gene (Adeno-LacZ) and with the S16EPLN gene (Adeno-S16EPLN) were prepared as previously described (6).

**Generation of MI rats.** When the rats were 7–8 weeks old, left coronary artery ligation was performed as previously described (20). Briefly, rats were anesthetized with ketamine (100 mg/kg) and xylazine (10 mg/kg), endotracheally intubated, and mechanically ventilated with room air (respiratory rate 55–65 breaths per minute, tidal volume 2.5 ml). Under sterile conditions, a left anterior thoracotomy was performed to expose the heart. The left anterior descending coronary artery was ligated between the right ventricular outflow tract and the left atrium with a 6-0 silk suture that was passed through the superficial layers of myocardium (20). The lungs were then reinflated and the chest incision closed. Sham-operated rats (no-MI rats) were prepared in the same manner but did not undergo coronary artery ligation.

**Randomization of MI rats for gene transfer.** At 5 weeks after coronary ligation, following echocardiographic determination of cardiac function and MI size, animals with an infarct size between 30% and 40% were randomized into two groups: rAAV-S16E gene transfer (MI-S16EPLN) and saline injection (MI-saline). In the MI-saline group, a volume of saline alone equal to that of the virus solution was injected with the same procedures for gene transfer used in the MI-S16EPLN group.

**Echocardiography.** Echocardiograms to assess LV size and function were recorded as previously described (21) at 5 weeks after coronary occlusion (before randomization) and at 2 months and 6 months after the gene transfer procedure. Light anesthesia was induced with intraperitoneal ketamine (50 mg/kg) and xylazine (5 mg/kg). Two-dimensional parasternal long-axis images were obtained perpendicular to the short axis and were deemed appropriate at the site where LV length was maximum and both mitral and aortic valves were contained in the image. The LV endocardial border was manually traced, and long-axis dimensions and LV areas at end-systole and end-diastole were determined. The LV end-diastolic volume (LVEDV), LV end-systolic volume (LVESV), and LV ejection fraction (LVEF) were calculated using the area-length method, which has been validated in rodents and humans (22). Three investigators blinded as to experimental groups agreed on the optimal echo frame for visualizing the left ventricle in the two-dimensional long-axis view at each time point. The frames selected were then analyzed in a random, blinded manner by two experienced investigators. The means of the differences between these two investigators were  $0.001 \pm 0.047$  ml ( $\pm$  SD) for LVEDV,  $0.005 \pm 0.032$  ml for LVESV, and  $0.297 \pm 2.27\%$  for LVEF. After completion of two-dimensional imaging, pulse-wave Doppler interrogation of mitral flow was performed in a parasternal long-axis view in order to evaluate diastolic filling; the ratio of early mitral orifice inflow velocity (E) to inflow velocity during atrial contraction (A) was calculated (23).

In this study, in which treatment was expected to alter LV remodeling, it was necessary to have a reliable estimate of the extent of the completed MI relative to the LV size prior to randomization into treated and untreated groups. Therefore an initial study was done in a separate group of ten rats, comparing echocardiographic and post-mortem histological methods. Myocardial infarct size was estimated by the centerline method (24) (which measures wall excursion at 100 points around the LV circumference) in two-dimensional short-axis images at three LV levels (mid-papillary muscle, chordae tendinae, and near the apex), and the size estimates at the three levels were averaged to determine the percentage of the LV circumference that demonstrated systolic akinesis or dyskinesis. Values obtained by this method were compared with those obtained by histological quantification (25) at these three regions; a highly significant correlation was found ( $r^2 = 0.948$ ,  $P < 0.01$ ), and the mean of the differences in infarct size between the two methods was  $0.10 \pm 2.98\%$  ( $\pm$  SD).

**Gene transfer.** The gene transfer procedure in normal and MI rats was developed through modifications of our hamster gene transfer protocol (6). Briefly, animals were anesthetized with sodium pentobarbital (70 mg/kg intraperitoneally), intubated, and ventilated. A small left anterior thoracotomy was performed, and string occluders were placed loosely around the ascending aorta and main pulmonary artery. A PE-60 catheter (Becton Dickinson and Co., Sparks, Maryland, USA) was then inserted through the right carotid artery into the aortic root just above the aortic valve and below the occluder for measurement of pressure and for injections, and the animals were then subjected to general hypothermia by external cooling with ice packs to below  $26^{\circ}\text{C}$ . The great vessels (pulmonary artery followed by aorta) were then occluded. Next, 0.4 ml of cardioplegic solution (6) was injected through the aortic catheter, followed by 0.4 ml of cardioplegic solution containing 10  $\mu\text{g}$  of substance P (26), and, after 60 seconds, 2.0 ml of cardioplegic solution containing 5  $\mu\text{g}$  of substance P and the viral vector was delivered. The occlusions were released 90 seconds later, dobutamine was administered, and the animals were rewarmed.



In preliminary studies, Adeno-LacZ with  $1.7 \times 10^6$  to  $4.0 \times 10^6$  virus particles per gram body weight and rAAV-LacZ with  $2.0 \times 10^6$  genome copies per gram body weight were evaluated for LacZ marker gene expression at 4 days and 5 weeks, respectively, after gene transfer by  $\beta$ -gal staining performed in three transverse cardiac sections per animal. The percentage of  $\beta$ -gal-positive myocytes was determined as previously reported in our laboratory (6). During these preliminary studies, the optimal volume of the solution containing cardioplegic solution, substance P, and viral vector was assessed. The highest efficiency was achieved with the largest volume tested, 2.0 ml, which was then used in the randomized studies in which rAAV-S16EPLN ( $1.9 \times 10^6$  genome copies per gram body weight) or saline was administered in the MI rats.

**Hemodynamic measurements.** At 6 months after gene transfer, immediately after the final echocardiographic study, hemodynamic measurements were performed. A 2-French catheter-tip pressure transducer catheter (SPR-407; Millar Instruments Inc., Houston, Texas, USA) was introduced into the left ventricle through the right carotid artery (proximal to the site of prior catheter insertion for gene transfer) for measurements of LV pressures, and contractility and relaxation were assessed by maximum and minimum first derivatives of LV pressure (LV dP/dt) and  $\tau$ , the time constant of relaxation (using an exponential function), as previously described (21). After base-line measurements, each animal underwent stepwise dobutamine infusions ( $0.75$ – $4 \mu\text{g/kg/min}$ ) with data recordings at steady state at each dose.

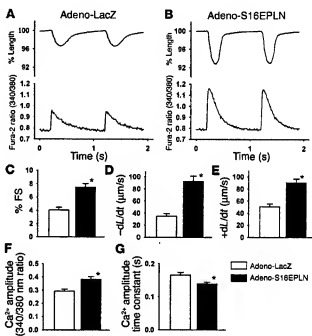
Meridional stress of the LV wall at peak-systole and end-diastole was estimated, using non-simultaneous data, as  $PR_i + 2b(1 + b/2R_i)$ , where  $P$  is LV pressure,  $R_i$  is inner LV minor-axis radius, and  $b$  is the mean of anterior and posterior wall thickness values (21).

**Histological analysis.** For morphometric analysis, LV specimens were fixed with 10% buffered formalin and embedded in paraffin. Several sections were prepared from each specimen and stained with H&E for assessment of myocardial cellular infiltrates and inflammation, and with Masson's trichrome stain to assess the area of fibrosis using a point-counting method (27). Myocyte diameters were measured as previously described (28). In brief, in the sections stained with H&E, a total of 100 myocardial cells were randomly selected from the noninfarcted area from each animal, and the shortest diameters of transversely cut fibers were measured at the level of the nucleus with the aid of an image analyzer (LUZEX 3U; Nikon Corp., Tokyo, Japan). This method was used to minimize errors in comparing different tissue sections for estimation of the size of cardiomyocytes, since slight offset can occur in transverse sectioning.

**Western blot analysis.** SR microvesicles were isolated from the non-infarcted posterior-lateral region of the left ventricle by sequential centrifugation as previously described (29). Protein concentration was determined by the bicinchoninic acid assay (Pierce Chemical Co., Rockford, Illinois, USA) using BSA as standard. Twenty micrograms of protein was electrophoresed on 4–12% polyacrylamide gels and transferred to PVDF membranes (Bio-Rad Laboratories Inc., Hercules, California, USA). Membranes were incubated with primary antibodies for 1 hour at room temperature and then with appropriate HRP-conjugated secondary antibodies. The immune complexes were detected with a chemiluminescence kit (Pierce Chemical Co.). The primary antibodies were anti-PLN (clone A1; Upstate Biotechnology Inc., Lake Placid, New York, USA), anti-SERCA2 (Affinity BioReagents Inc., Golden, Colorado, USA), and anti-phospho-PLN (Ser16) (Upstate Biotechnology Inc.).

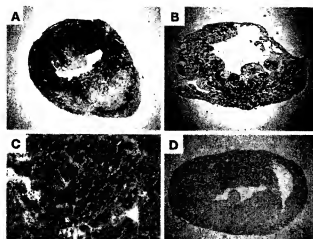
The endogenous wild-type PLN and the S16EPLN transgene were measured using *in vitro* phosphorylation followed by immunoblotting, as previously described (7). Briefly, the protein samples were treated with protein kinase A to saturate the level of phosphorylation reaction and then subjected to immunoblotting. An anti-phospho-PLN (Ser16) antibody was used to measure the endogenous wild-type PLN that could be phosphorylated. It should be noted that, although S16EPLN was designed as a pseudophosphorylated PLN mutant, it is not detectable with the anti-phospho-PLN (Ser16) antibody. On the other hand, the anti-PLN antibody used in this study recognizes both S16EPLN and the wild-type PLN with equivalent sensitivities and was used to determine the sum of the S16EPLN transgene and the endogenous wild-type PLN. The level of the S16EPLN was estimated by the difference between total amount of PLN and the level of PLN that was phosphorylated to the level of saturation by protein kinase A.

**Demonstration of S16EPLN effectiveness in rat cardiomyocytes.** To establish that the rat heart responds to S16EPLN in a manner similar to



**Figure 1**

Enhanced shortening and SR calcium cycling in isolated adult rat cardiomyocytes treated with S16EPLN. Ventricular cardiomyocytes were isolated from adult Wistar rats according to the protocol described by Zho et al. (30). Cells were transfected with adenoviral vectors expressing LacZ (Adeno-LacZ) or S16EPLN (Adeno-S16EPLN) at a multiplicity of infection of 100 and cultured for 36 hours. Nearly 100% efficiency of transfection was confirmed by  $\beta$ -gal staining of Adeno-LacZ-treated cells. Thereafter, both Adeno-LacZ-treated cells and Adeno-S16EPLN-treated cells were loaded with fura-2/AM, and cell shortening and changes in intracellular calcium concentration were monitored. (A and B) Representative tracings of cell length and fura-2 340/380 ratio, an index of calcium concentration. (C–E) Indices of cell shortening (percentage fractional shortening [% FS] and  $-dL/dt$ ) and relaxation ( $+dL/dt$ ). (F and G) The averaged peak amplitude of an index of calcium transient (F) and the averaged decay time constant of the descending limb of calcium transient (G). Data represent mean  $\pm$  SE and are accumulated from five independent experiments from five animals. A total of 40 cells were measured for each treatment group. \* $P < 0.05$  between groups. L, length.

**Figure 2**

Representative images of  $\beta$ -gal activity in normal and MI rat LV slices after LacZ marker gene transfer. (A and B) High-efficiency cardiac gene transfer is shown in normal rats (A) and MI rats (B) at 4 days after Adeno-LacZ transfer. (C and D) Significant inflammatory responses are evident in MI rats at 5 weeks after rAAV-LacZ transfer. (C) H&E staining. (D)  $\beta$ -gal staining. Magnifications: A, B, and D,  $\times 4.5$ ; C,  $\times 200$ .

that of other species, an adenovirus vector carrying S16EPLN was transfected in isolated normal adult rat cardiomyocytes for 36 hours (30), and cell contraction and  $Ca^{2+}$  transients were measured using an edge-motion detector and a dual-excitation spectrofluorometer (IonOptix Corp., Milton, Massachusetts, USA) as previously described (31). An enhanced peak  $Ca^{2+}$  transient in systole and a decrease in the time constant of  $Ca^{2+}$ -transient decay ( $\tau$ ) were noted accompanying clearly enhanced cell shortening and relaxation (Figure 1).

In addition, the same adenovirus vector was transferred *in vivo* in normal rats using the transcatheter gene transfer procedure. Four days after gene transfer, the animals were subjected to echocardiography. Increased percentage fractional shortening (S16EPLN-treated,  $47.2 \pm 0.6$ ; saline-treated,  $39.0 \pm 1.4$ ;  $n = 6$  each;  $P < 0.05$ ) and slightly smaller LV diastolic chamber size (LV end-diastolic diameter: S16EPLN-treated,  $7.40 \pm 0.12$  mm; saline-treated,  $8.02 \pm 0.16$  mm;  $n = 6$  each;  $P < 0.05$ ) were observed with short-term S16EPLN treatment. Hemodynamic analysis of the same animals showed a trend toward augmentation of positive maximum LV  $dP/dt$  by S16EPLN treatment (S16EPLN-treated,  $7,069 \pm 456$  mmHg/s; saline-treated,  $6,260 \pm 299$  mmHg/s;  $n = 6$  each), which did not reach statistical significance ( $P = 0.164$ ).

**Statistical analysis.** All values are expressed as mean  $\pm$  SE unless specified otherwise. The significance of the differences between group means for most data was analyzed by one-way ANOVA with post hoc comparisons by the Student-Newman-Keuls test. For serial echocardiographic data, the main effects of treatment were tested using two-factor ANOVA for repeated measures, and differences between the groups at specific time points were assessed using two-factor ANOVA with post hoc comparisons by the Student-Newman-Keuls test. A value of  $P < 0.05$  was considered statistically significant.

## Results

**Establishment of *in vivo* high-efficiency gene delivery in MI rats.** Representative images stained for  $\beta$ -gal activity of normal and MI rat hearts are shown in Figure 2. Overall, in initial studies using Adeno-LacZ, the transduction efficiency was  $55.3\% \pm 2.3\%$  (range,  $33.2$ – $81.7\%$ ) of LV in seven normal rats (Figure 2A) and  $40.1\% \pm 2.3\%$  (range,  $23.2$ – $62.5\%$ ) of LV in the noninfarcted regions of the heart in nine MI rats (Figure 2B). A range of viral-injectate volumes was studied, and since the highest efficiency (61.2%) was associated with the highest volume of injectate (2.0 ml) in MI rats, this volume was used in subsequent studies.

At 5 weeks after the transfection of rAAV-LacZ ( $n = 6$ ), heavy inflammation with diffuse monocyte infiltration was observed in the LV of normal and MI rats (Figure 2C), and less than 1% of myocytes were positively stained for  $\beta$ -gal activity (Figure 2D). In contrast, inflammatory changes were not observed in rats that received the rAAV-S16EPLN vector over 6 months (data not shown).

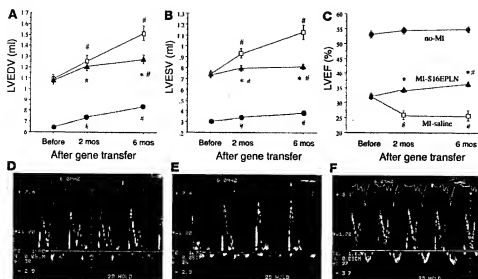
**Pre-gene transfer development of heart failure in MI rats.** The coronary artery was ligated in 113 rats, of which 40 died in the first 48 hours (early mortality 35.4%) and two died within 5 weeks (late mortality 1.8%). Among the 71 survivors at 5 weeks after MI, the infarct size assessed by echocardiography was 30–40% in 34 rats, and these animals were randomized into two groups (MI-S16EPLN and MI-saline) prior to the gene transfer procedure; thus, 22 rats with small ( $<30\%$ ) infarctions and 15 rats with very large ( $>40\%$ ) infarctions were excluded from the study. A group of age-matched sham-operated (no-MI) rats was also studied ( $n = 13$ ). In all randomized MI rats, LV function was significantly depressed and LVEDV increased compared with no-MI rats, and there were no significant differences in LV size and function, or in infarct sizes, between the two randomized treatment groups prior to treatment (Table 1). In the subsequent gene transfer procedure, perioperative mortality (within 24 hours after surgery) was 14.7%, with 13 survivors in the MI-S16EPLN group and 16 survivors in the MI-saline group.

**Improvement of cardiac function, contractility, and suppression of global remodeling by rAAV-S16EPLN treatment in rats with post-MI heart failure.** Four rats (19%) in the MI-saline group died with signs of heart failure

**Table 1**  
Base-line echocardiographic characteristics of MI rats before gene transfer

	No-MI	After MI (5 weeks)	
		MI-saline	MI-S16EPLN
Number	13	16 (12) <sup>a</sup>	13 (12) <sup>a</sup>
Body weight (g)	$428 \pm 12$	$408 \pm 8$	$415 \pm 8$
Infarct size (%)	—	$37.1 \pm 0.65$	$36.7 \pm 0.73$
Heart rate (bpm)	$279 \pm 6$	$292 \pm 6$	$279 \pm 4$
LVEF (%)	$53.1 \pm 1.0$	$32.4 \pm 0.5^b$	$32.4 \pm 1.0^b$
LVEDV (ml)	$0.68 \pm 0.03$	$1.06 \pm 0.03^a$	$1.07 \pm 0.04^a$

<sup>a</sup>Immediate survivor (survived 6 months after gene transfer). <sup>b</sup> $P < 0.05$  vs. no-MI. bpm, beats per minute.

**Figure 3**

Serial changes of echocardiographic variables before and after S16EPLN gene transfer. (A) LVEDV, (B) LVESV, (C) LVEF. The S16EPLN treatment enhanced LV contractility and suppressed LV dilation over 6 months. Values are mean  $\pm$  SE. \* $P < 0.05$ , MI-S16EPLN vs. MI-saline animals. # $P < 0.05$  vs. before gene transfer. Circles, no-MI; squares, MI-saline; triangles, MI-S16EPLN. (D–F) Representative images of pulse-wave Doppler recordings of mitral flow at 6 months in no-MI (D), MI-saline (E), and MI-S16EPLN rats (F).

(e.g., peripheral edema, respiratory distress, and general fatigue), one at 2 months, one at 2.5 months, and two at 5.5 months after gene transfer, whereas one rat (7.7%) in the MI-S16EPLN group died at 4 months of an unknown cause, without signs of heart failure. There was no death in the no-MI group.

By serial echocardiography in MI-saline rats, the LVEF progressively decreased (by 20.0%) from pre-gene transfer base line, and LVEDV increased substantially (by 38.4%) during the 6-month observation period (Figure 3, A and C). In no-MI rats, the LVEF did not change and the LVEDV increased moderately, paralleling natural growth. In contrast, the rAAV-S16EPLN treatment increased LVEF by 6.0% at 2 months and by 12.8% at 6 months compared with base line (Figure 3C). The LVEDV increased somewhat in the MI-S16EPLN animals; however, the extent of change (by 18.2% at 6 months after gene transfer compared with pre-gene transfer base line) was 53.4% less than that occurring in the MI-saline group and was comparable to that in the no-MI animals (Figure 3A).

Improvement of diastolic LV function was shown in the MI-S16EPLN versus the MI-saline group using pulse-wave Doppler recordings of mitral inflow. Increased early filling velocity (E) and decreased late filling velocity (atrial contraction; A), which are characteristic of failing hearts with elevated LV filling pressure, were observed in MI-saline rats (Figure 3E), whereas in the rAAV-S16EPLN-transferred group, the E/A ratio was lowered to near normal (Figure 3F). These and other selected echocardiographic data at 6 months are summarized in Table 2.

Improvement of hemodynamic LV function, assessed by systolic and diastolic LV pressures, contractility, and relaxation, was further confirmed by high-fidelity LV manometry at 6 months after S16EPLN treatment. In the MI-S16EPLN rats, the maximum LV  $dP/dt$  was significantly higher, and indices of relaxation (minimum  $dP/dt$  and  $\tau$ ) were enhanced compared with those in MI-saline animals (Table 3). Also, the LV end-diastolic pressure (LVEDP), which was considerably elevated in MI-saline rats, was near normal in the S16EPLN treatment group (Table 3). The responses to dobutamine, a  $\beta$ -adrenergic agonist, are shown in Figure 4. In the MI-saline group, contractility and relaxation measures (maximum and minimum LV  $dP/dt$  and  $\tau$ ) were severely blunted in response to dobutamine compared with those in the no-MI group. These variables

were markedly enhanced by  $\beta$ -adrenergic stimulation in the MI-S16EPLN group compared with those in the MI-saline group, with  $\tau$  being near normal at higher dobutamine doses (Figure 4). Estimates of both systolic and diastolic LV wall stress, which were markedly elevated in MI-saline animals, were largely suppressed in the MI-S16EPLN group (Table 3).

**Expression of SR  $Ca^{2+}$ -handling proteins.** The level of S16EPLN expression was estimated as previously described (7). S16EPLN transfer induced a 46% increase in total immunoreactive PLN (endogenous PLN and S16EPLN) compared with MI-saline. Endogenous PLN was approximately 10% decreased in S16EPLN-treated animals. The overall relative molecular ratio of the endogenous PLN versus S16EPLN was approximately 1:0.57 in the noninfarcted myocardium from the treatment group. S16EPLN transgene expression over 6 months was confirmed by RT-PCR (Figure 5A). RT-PCR was repeated using purified poly(A) RNA to further confirm that amplification was transcript dependent, and the results were similar (data not shown). The SERCA2 protein level was also estimated by immunoblotting and was by 42% higher in S16EPLN-treated ani-

**Table 2**  
Postmortem and echocardiographic analysis at 6 months after S16EPLN gene transfer

	No-MI	MI-saline	MI-S16EPLN
Number	13	12	12
BW (g)	646 $\pm$ 21	632 $\pm$ 13	649 $\pm$ 22
LW/BW	1.46 $\pm$ 0.07	1.83 $\pm$ 0.08 <sup>A</sup>	1.56 $\pm$ 0.07 <sup>A,B</sup>
RVW/BW	0.34 $\pm$ 0.02	0.51 $\pm$ 0.05 <sup>A</sup>	0.35 $\pm$ 0.02 <sup>A,B</sup>
LungW/BW	2.51 $\pm$ 0.09	3.46 $\pm$ 0.48 <sup>A</sup>	2.58 $\pm$ 0.12 <sup>B</sup>
Heart rate (bpm)	290 $\pm$ 9	282 $\pm$ 23	277 $\pm$ 8
LVEDV (ml)	0.84 $\pm$ 0.02	1.52 $\pm$ 0.07 <sup>A</sup>	1.28 $\pm$ 0.04 <sup>A,B</sup>
LVESV (ml)	0.38 $\pm$ 0.01	1.13 $\pm$ 0.07 <sup>A</sup>	0.81 $\pm$ 0.03 <sup>A,B</sup>
LVEF (%)	54.7 $\pm$ 1.0	25.8 $\pm$ 1.7 <sup>A</sup>	36.4 $\pm$ 0.8 <sup>A,B</sup>
E/A ratio	1.67 $\pm$ 0.05	2.32 $\pm$ 0.21 <sup>A</sup>	1.61 $\pm$ 0.05 <sup>B</sup>

<sup>A</sup> $P < 0.05$  vs. no-MI. <sup>B</sup> $P < 0.05$  vs. MI-saline animals. BW, body weight; LW, LV weight; RVW, right ventricular weight; lungW, lung weight; E/A ratio, Doppler-determined E/A ratio.

**Table 3**

Hemodynamic variables at 6 months after S16EPLN gene transfer

	No-MI	After MI	
		MI-saline	MI-S16EPLN
Number	9	9	8
Heart rate (bpm)	290 ± 9	282 ± 23	277 ± 8
PLVP (mmHg)	114.6 ± 4.7	105.8 ± 4.0	114.5 ± 3.9
Max dP/dt (mmHg/s)	7,949 ± 268	5,375 ± 439 <sup>A</sup>	6,824 ± 212 <sup>A</sup>
Min dP/dt (mmHg/s)	-6,734 ± 340	-3,971 ± 254 <sup>A</sup>	-5,468 ± 300 <sup>A</sup>
τ (ms)	13.7 ± 0.9	22.1 ± 1.0 <sup>A</sup>	17.9 ± 1.1 <sup>B</sup>
LVEDP (mmHg)	1.8 ± 0.6	13.4 ± 1.4 <sup>A</sup>	3.2 ± 0.4 <sup>B</sup>
Diastolic WS (kdyne/cm <sup>2</sup> )	1.05 ± 0.39	9.20 ± 1.06 <sup>A</sup>	2.88 ± 0.47 <sup>B</sup>
Systolic WS (kdyne/cm <sup>2</sup> )	24.7 ± 0.9	59.0 ± 3.5 <sup>A</sup>	46.1 ± 3.9 <sup>A,B</sup>

<sup>A</sup>P < 0.05 vs. no-MI, <sup>B</sup>P < 0.05 vs. MI-saline animals. PLVP, peak LV systolic pressure; max dP/dt, LV peak rate of change of pressure during isovolumic contraction; min dP/dt, LV peak rate of change of pressure during isovolumic relaxation; LVEDP, LV end-diastolic pressure; WS, meridional stress of LV wall; kdyne, kilodynes.

mals, most probably reflecting general improvement of cardiac function and suppressed ventricular remodeling.

**Suppression of chronic remodeling, fibrosis, and pulmonary effusion in MI animals by S16EPLN treatment.** Both the LV/body weight ratio and the right ventricular/body weight ratio were significantly increased in MI-saline rats compared with no-MI rats, and these values were much reduced in MI-S16EPLN rats compared with MI-saline rats (Table 2). The lung/body weight ratio was elevated in the MI-saline group and almost normal in the MI-S16EPLN group (Table 2).

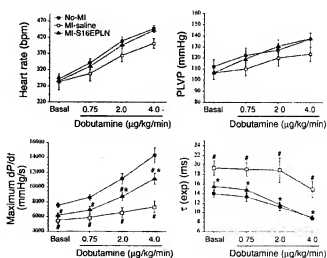
The S16EPLN treatment did not significantly affect changes in the thickness of infarcted LV wall between measurement before gene transfer and measurement 6 months after gene transfer. Changes in the diastolic ventricular anterior wall thickness, measured by M-mode echocardiography, were from 0.95 ± 0.04 mm to 0.89 ± 0.05 mm (± SE; n = 12) in S16EPLN-treated animals and from 0.98 ± 0.05 mm to 0.92 ± 0.04 mm (± SE; n = 12) in the saline-treated group. On the other hand, the degree of compensatory cardiomyocyte hypertrophy in the noninfarcted area of myocardium, assessed as cell diameter, was significantly lower in MI-S16EPLN rats than in MI-saline animals (Figure 5E). To test whether the transgene (S16EPLN) affected Ca<sup>2+</sup> signaling, which can be linked to cardiomyocyte hypertrophy (32, 33) through molecules such as calcium/calmodulin-dependent kinase II (CaMKII) (34) or calcineurin (35), we transfected cultured rat neonatal cardiomyocytes with an adenoviral vector carrying S16EPLN (AdV-S16EPLN) for 36 hours and treated them further with the Gq-coupled agonists phenylephrine and endothelin-1 for 24 hours. Thereafter, myofibrinogenesis was measured by phalloidin staining and immunostaining with an anti-myosin light chain antibody, and induction of atrial natriuretic peptide (ANP), an embryonic gene marker, was also assessed. S16EPLN overexpression did not induce hypertrophic changes, nor did it alter hypertrophy induced by Gq-coupled agonists in this cell type (data not shown).

The mRNA expression of ANP and skeletal actin was evaluated by Northern blot analysis in the MI rat hearts after gene transfer treatment. Although there was a trend toward suppression of these marker genes in the S16EPLN-treated hearts, quantitative measurement of signal intensity did not reach statistical significance because of specimen-dependent variation in both saline-treated and S16EPLN-treated groups (data not shown).

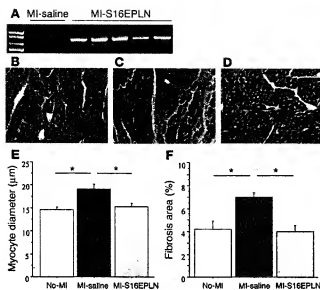
In quantitative histological analysis, a significantly lower extent of interstitial fibrosis was apparent in the noninfarcted region in the S16EPLN-treated animals versus the MI-saline group (Figure 5F). Histological studies prior to gene transfer were not included in this study, since biopsy would have been required. However, histological evaluation of the noninfarcted LV posterior wall collected from the operated rats in a separate study, which had similar myocardial-infarct sizes, showed only mild signs of fibrosis at 5 weeks after the coronary artery ligation procedure (data not shown).

## Discussion

The findings of this study of a postinfarction rat model with established heart failure demonstrate that in vivo delivery of the S16EPLN gene was highly effective in improving LV function and mitigating adverse remodeling compared with delivery of saline by the same route. LV function, measured by echocardiography, was enhanced in the S16EPLN-treated group, as evidenced by higher LVEF, which was due, at least in part, to reduced afterload (reduced systolic wall stress). In addition, the mutant protein increased contractility, and the positive inotropic effect (increased maximum LV dP/dt) also was associated with marked improvement in LV relaxation (enhanced minimum LV dP/dt and shortened τ). LV dP/dt is known to be influenced by myocardial contractility and also varies directly with the preload (36), but it is considered to be largely independent of afterload, provided the peak occurs at or before opening of the aortic valve (which was the case in these experiments). Therefore, the finding that this measure was significantly higher in the S16EPLN-treated group than in untreated controls despite lower preload (LVEDP, LVEDV, and diastolic wall stress) indicates that treatment enhanced LV contractility. Diastolic function also was improved by treatment: the E/A ratio was lowered, and LVEDP and diastolic wall stress were nearly normalized. Importantly, unfavorable LV remodeling was largely prevented by rAAV-S16EPLN treatment; this was reflected by limitation of LV dilation and reduction of LV hypertrophy (LV

**Figure 4**

Responses to β-adrenergic agonist stimulation in rAAV-S16EPLN-treated versus MI-saline rats at 6 months after gene transfer. \*P < 0.05, MI-S16EPLN vs. MI-saline animals. <sup>†</sup>P < 0.05, MI-S16EPLN or MI-saline vs. no-MI animals. PLVP, peak LV systolic pressure. exp, exponential.

**Figure 5**

S16EPLN transgene expression and suppression of histological signs of cardiac remodeling after S16EPLN gene transfer. (A) RT-PCR confirmation of transgene expression in noninfarcted myocardium isolated from S16EPLN-treated hearts at 6 months after gene transfer. Extracted RNA was treated with DNase before RT-PCR. Primers were designed within 5' noncoding and 3' noncoding sequences in rAAV-S16EPLN vector, flanking the S16EPLN cDNA coding sequence. (B–D) Representative images of Masson's trichrome staining (x200): no-MI (B), MI-saline (C), and MI-S16EPLN animals (D). (E and F) Myocyte diameters (E) and fibrosis areas (F) were quantitatively analyzed as described in Methods. Studies occurred at 6 months after gene transfer. Data represent mean  $\pm$  SE. \* $P < 0.05$  between groups ( $n = 5$  per group).

weight and cardiomyocyte size). The right ventricular weight also was significantly lower in the treated group, suggesting that lowered LVEDP led to reduced pulmonary artery and right ventricular pressures (although right heart pressures were not measured). The reduction of the wet lung/body weight ratio with S16EPLN treatment suggests that lowered LVEDP also led to improved pulmonary capillary pressure and reduced lung edema.

We obtained relatively specific cardiac gene expression, even though the CMV promoter is not tissue specific. This can be attributed primarily to the transcoronary delivery of the vector during occlusion of the aorta distal to the site of vector injection (which prevented systemic delivery), and the simultaneous occlusion of the pulmonary artery (which prevented delivery to the lungs). In a previous study using the same gene transfer method in hamsters (7), we observed only occasional cells with minimal  $\beta$ -gal staining in the liver and ascending aorta, and no cells with  $\beta$ -gal staining in the brain, liver, spleen, kidney, and lung. We were unable to perform a similar analysis in the present study because of the immune reaction caused by the rAAV-LacZ treatment. In histological examination, we have reevaluated rAAV-LacZ-transferred hamster myocardium, searching for  $\beta$ -gal-positive staining in the coronary vascular bed and in the perivascular interstitial area, and we observed none. Lack of vascular gene expression after the transcoronary perfusion of rAAV vectors was independently reported by Xiao's group (37). Thus, we speculate that S16EPLN expressed in cardiomyocytes exerted beneficial effects in the failing heart.

Cardiac remodeling after MI includes infarct expansion and eccentric hypertrophy of the noninfarcted left ventricle of the volume-overload type. Eccentric hypertrophy is characterized by progressive chamber dilation and an increase in the ratio of chamber volume to wall thickness (20), a setting that eventually leads to decreased myocardial function and increased myocardial fibrosis (38). Pharmacological approaches in patients with heart failure, such as inhibition of angiotensin-converting enzyme and use of ventricular-assist devices, have demonstrated that remodeling can be a partly reversible process (so-called reverse remodeling) (39); ventricular-assist devices can produce especially marked reverse remodeling (40). In the current study, the randomization and gene transfer were performed at 5 weeks after coro-

nary occlusion, when expansion and scarring of the infarct are nearly complete (41). The infarct size was closely comparable at randomization in S16EPLN-treated and control saline-treated groups, and the success of the randomization is further indicated by the closely comparable echocardiographic measurements of LV size and function in the two groups before the gene transfer procedure. On the other hand, postmortem infarct size was not an endpoint measure of this study, since infarct size is expressed relative to the size of the left ventricle, and we expected, and found, substantial differences in remodeling of the surviving myocardium between treated and untreated groups.

It is of interest that the favorable global actions of the S16EPLN gene in the heart occurred despite a limited transcoronary transduction efficiency, which is estimated at 60% or less of the cell population in the noninfarcted myocardium, based on the initial LacZ expression studies. We attribute these effects on global function, including enhanced  $\beta$ -adrenergic responses found on hemodynamic analysis, in part to reduced loading on the left ventricle in the S16EPLN-treated group, indicated by reduction of the estimated end-systolic and end-diastolic wall-stress values. A decrease in wall stress has favorable effects on remodeling of noninfarcted remote myocardium, a process that may involve apoptotic cell loss (42, 43). It is also possible that lowered wall stress, particularly in diastole, could have reduced subendocardial ischemia, if present, by improving myocardial blood flow to the inner LV wall, thereby improving cardiac function (44). In a study of sustained aortic stenosis in PLN-null mice by Kiriazis et al. (15), a relatively greater pressure gradient across the banding might have contributed to the trend of greater incidence of heart failure in that group of mice. On the other hand, in the MLP cardiomyopathic mouse model, evidence suggested that wall-stress reduction, which was achieved by PLN ablation, prevents development of heart failure by maintaining structural and functional integrity of the Z-disc/titin complex (45). Abnormalities of this complex also may occur in a recently identified subset of patients with dilated cardiomyopathy who harbor mutations in the telethonin-interacting domain of MLP, telethonin being a titin-binding molecule (45). We postulate that S16EPLN-treated MI rats had more favorable loading on all the cells, both S16EPLN-transfected and nontransfected cardiomyocytes, in the noninfarcted

region of the left ventricle, and that systolic unloading due to enhanced contractility of transfected cells contributed to a reduction of end-systolic volume and a higher ejection fraction. Diastolic unloading due to improved relaxation and lower end-diastolic LV volume contributed to enhanced diastolic function and reduction of unfavorable remodeling.

In a recent report, the effects of PLN ablation, produced by crossbreeding with PLN-null mice, were assessed in two genetic mouse models, Gtg overexpression and targeted mutation of myosin-binding protein C, both of which exhibited extensive cardiomyopathic changes associated with the development of cardiac dysfunction and dilation (14). No effect of PLN ablation on echocardiographic measures of hypertrophy and dysfunction were observed in either model, and impaired hemodynamic responsiveness to  $\beta$ -adrenergic stimulation was not affected (14). These findings contrast with those of our previous study on PLN ablation in MLP cardiomyopathic mice (using a similar crossbreeding approach), in which the cardiomyopathic phenotype did not develop (12), and they also differ from the present findings in the adult rat with MI, in which an entirely different approach was used to achieve PLN inhibition in the presence of established cardiac dysfunction and dilation.

It seems possible that in the two transgenic models described above (14), the strong genetic stimuli mediating cardiomyopathic changes, present in utero and thereafter, may have overshadowed the effect of PLN ablation to enhance cardiomyocyte contractility. In the MLP cardiomyopathic model, on the other hand, cardiac dilation and hypertrophy develop progressively over several weeks after birth (45, 46), and in that setting, correction by PLN ablation of the  $\text{Ca}^{2+}$  handling defect during postnatal cardiac growth may explain the observed complete prevention of the dilated cardiomyopathy phenotype (12). Thus, we postulate that enhanced cardiac function maintained normal heart size, obviating the progressive cardiac dilation associated with increased wall stress and secondary cardiac hypertrophy present in MLP-null mice (47).

Recently, an R9C mutation of PLN was identified in patients with familial cardiomyopathy (16), and suppression of Ser16 phosphorylation of wild-type PLN was proposed as the mechanism of the dominant negative effect of this mutation (16). The R9C PLN itself also lacks the ability to phosphorylate Ser16. This finding supports our concept that overexpression of the pseudophosphorylated form of PLN (S16EPLN) has the opposite effect, leading to a chronic beneficial effect on the failing myocardium. On the other hand, in another recent study, an L39stop mutation in PLN in patients with hereditary cardiomyopathy was reported to represent a possible long-term adverse effect of innate absence of PLN (17). The precise role of the L39stop mutation in humans remains to be clarified, since the unstable truncated L39stop PLN peptide contains a portion of the cytoplasmic inhibitor domain of PLN that could inhibit SERCA2 (47).

PLN is an endogenous muscle-specific inhibitor of SERCA2, and the regulation of its inhibitory function is mainly via its phosphorylation by cAMP-dependent protein kinase at Ser16, and also by CaMKII (48) at Thr17. Cardiac-specific disruption of PLN in mice results in a marked increase in myocardial contractility, without change in the maximum cardiac response to  $\beta$ -adrenergic stimulation (48). CaMKII-dependent phosphorylation of PLN may contribute to a positive force-frequency relationship and to frequency-dependent acceleration of relaxation (49), although Bers's group has recently reported that the latter event might be at least partly independent of PLN (50). As potential therapeutic strategies for heart

failure, two approaches have been employed to enhance the reuptake of  $\text{Ca}^{2+}$  into the cardiac SR through this mechanism: alteration of the PLN/SERCA2 molecular ratio, and reduction of PLN activity. These approaches have included gene transfer of SERCA2 (10, 51), use of antisense PLN RNA (52–54), a single peptide antibody designed against PLN (55), and overexpression of mutant forms of PLN to interfere with the interaction of SERCA2 and endogenous PLN (7, 12, 53) – an approach we initially used in cardiomyopathic hamsters *in vivo* (7). In our study in cardiomyopathic hamsters, however, the rapid deterioration of function, myocyte loss, and increasing fibrosis that occur consequent to the absence of  $\delta$ -sarcoglycan in this genetic form of cardiomyopathy (21, 56) limited long-term beneficial effects. Therefore, in the present study, we applied rAAV-S16EPLN gene therapy in the rat post-MI model of chronic heart failure, in which sustained overload on noninfarcted regions is the major factor in the chronic progression of heart failure.

Our finding that  $\beta$ -adrenergic responsiveness to dobutamine was well maintained after gene transfer of S16EPLN may reflect the less marked heart failure in the treated group. This finding suggests that such treatment could enhance effects of sympathetic neurohormonal activation during exercise to increase cardiac function, acting in part by amplification of the force-frequency effect produced by  $\beta$ -adrenergic stimulation, which is reduced or absent in heart failure (57). Long-term inhibition of PLN also might lead to more effective adjunctive use of other therapies.

The single-stranded DNA virus vector rAAV is widely regarded as nonpathogenic and can achieve long-term gene expression in a variety of cell types, including myocytes (7, 58). The reason for the marked late cardiac inflammatory reaction to rAAV-LacZ and associated low efficiency of gene expression in rats after 5 weeks of gene transfer is not completely clear. Different preparations of rAAV-LacZ and an rAAV vector carrying an enhanced GFP reproducibly provoked similar tissue reactions, and we also found the reaction to occur in a different subspecies of rat (data not shown). The virus itself did not appear to be involved, since no signs of inflammatory reaction were evident in the rAAV-S16EPLN-treated group over 6 months. Therefore, we suspect that an immunoreaction to LacZ and enhanced GFP, which are completely foreign proteins to rats, was responsible, since S16EPLN is a minimally modified peptide derived from the native human PLN. Others have described high local efficiency of rAAV-LacZ transduction at 8 weeks in rats after direct intramyocardial injection, with no report of an immune response to LacZ (59). On the other hand, immunoreaction to foreign genes, such as LacZ, can occur in mice under certain circumstances (60). Species differences in immunoreactivity to rAAV-LacZ are suggested by our finding of no immunogenic reaction in a reexamination of cardiomyopathic hamster hearts in our previous study (7).

We consider that rAAV-S16EPLN could be an ideal vector for therapeutic use (5), not only because of its beneficial physiological effects and long-term action, but also because of its minimal modification from native PLN. It also has the advantage that LV contraction is enhanced in the absence of  $\beta$ -adrenergic receptor stimulation at rest, and without the sustained increase of intracellular cAMP that is associated with the chronic use of most positive inotropic agents, which have generally produced deleterious effects including increased mortality in patients with chronic heart failure (61). In this regard, ryanodine receptor phosphorylation induced by cAMP-dependent kinase in failing hearts may cause diastolic  $\text{SR Ca}^{2+}$  leakage, and associated malignant arrhythmia (62). The present study was powered in terms of numbers of rats to detect significant difference in cardiac function

and remodeling between groups at 6 months, followed by a terminal hemodynamic study, so that longer follow-up is not currently available. The degree of LV dilation may be the most powerful predictor of long-term prognosis in patients after MI (63), and additional studies on rats with heart failure after MI using larger numbers of animals and longer follow-up should clarify the effects of PLN inhibition on arrhythmias and survival. One animal died in the S16EPLN-treated group without evidence of heart failure. Although the difference in mortality was significant by preliminary Kaplan-Meier analysis, the numbers are inadequate to prove an effect of PLN inhibition in a formal survival analysis. S16EPLN-treated animals did not develop ventricular premature contractions either during repeated echocardiographic observations or during the final hemodynamic studies with intravenous catecholamine administration. Nevertheless, we recognize the possibility that S16EPLN treatment might induce arrhythmias in longer-term studies.

Our findings of enhanced function, reduced remodeling and fibrosis, and lessened heart failure in an animal model relevant to the setting of heart failure in patients after a large acute MI lend support to the potential therapeutic usefulness of this gene transfer approach. In addition, these studies document that the therapeutic

effects of PLN inhibition can be extended to acquired forms of heart failure, suggesting that previous results in some genetic models (7, 12) may be generalizable.

## Acknowledgments

We acknowledge partial fellowship support for Y. Iwanaga from NicOx SA and for T. Dierle from the Swiss National Science Foundation and the Freiwilrige Akademische Gesellschaft (Basel, Switzerland). General support was provided by the Leducq Foundation and by grant HLS3773 from the National Heart, Lung, and Blood Institute.

Received for publication May 20, 2003, and accepted in revised form December 28, 2003.

Address correspondence to: John Ross, Jr., Department of Medicine, University of California, San Diego, 9500 Gilman Drive, La Jolla, California 92093-0613B, USA. Phone: (858) 822-2267; Fax: (858) 534-1626; E-mail: jross@ucsd.edu.

Yoshiraka Iwanaga's present address is: Research Institute, National Cardiovascular Center, Osaka, Japan.

- Cohn JN, et al. 1997. Report of the National Heart, Lung, and Blood Institute Special Emphasis Panel on Heart Failure Research. *Circulation*. 95:766-770.
- Hosenpud JD, Bennett LE, Keck BM, Boucek M, et al. 1997. The Registry of the International Society for Heart and Lung Transplantation: eighteenth Official Report. *J Heart Lung Transplant*. 20:805-815.
- Hoshijima M, and Chien KR. 2002. Mixed signals in heart failure: cancer rules. *Clin Invest*. 109:849-855. doi:10.1172/CJ200215380.
- Chien KR. 1999. Stress pathways and heart failure. *Circ*. 98:555-558.
- Somja N, and Verma LM. 2000. Gene therapy: trials and tribulations. *Nat Rev Genet*. 1:91-99.
- Ikeeda Y, et al. 2002. Restoration of deficient membrane proteins in the cardiomyopathic hamster by in vivo cardiac gene transfer. *Circulation*. 105:502-508.
- Hoshijima M, et al. 2002. Chronic suppression of heart failure progression by a pseudophosphorylated mutant of phospholamban via in vivo cardiac rAAV gene delivery. *Nat Med*. 8:864-871.
- Marx SO, et al. 2000. PKA phosphorylation dissociates PKB12.6 from the calcium release channel (ryanodine receptor): defective regulation in failing hearts. *Cell*. 101:365-376.
- Morgan JP, Berry RE, Allen PD, Grossman W, and Gwathmey JK. 1990. Abnormal intracellular calcium handling, a major cause of systolic and diastolic dysfunction in ventricular myocardium from patients with heart failure. *Circulation*. 81:1121-1132.
- del Monte F, et al. 2001. Improvement in survival and cardiac metabolism after gene transfer of sarcolemmal calcium (Ca<sup>2+</sup>)-ATPase in a rat model of heart failure. *Circulation*. 104:1424-1429.
- Shah AS, et al. 2001. In vivo ventricular gene delivery of a beta-adrenergic receptor kinase inhibitor to the failing heart reverses cardiac dysfunction. *Circulation*. 103:1311-1316.
- Minamizawa S, et al. 1999. Chronic phospholamban-sarcoplasmic reticulum calcium ATPase interaction is the critical calcium cycling defect in dilated cardiomyopathy. *Cell*. 99:313-322.
- Freeman K, et al. 2001. Alterations in cardiac adrenergic signaling and calcium cycling differentially affect the progression of cardiomyopathy. *J Clin Invest*. 107:967-974.
- Song Q, et al. 2003. Rescue of cardiomyocyte dysfunction by phospholamban ablation does not prevent ventricular failure in genetic hypertrophy. *J Clin Invest*. 111:859-867. doi:10.1172/JCI200316738.
- Kiriazis H, et al. 2002. Hypertrophy and functional alterations in hyperdynamic phospholamban-knockout mouse hearts under chronic aortic stenosis. *Cardiovasc Res*. 53:372-381.
- Schmitt JP, et al. 2003. Dilated cardiomyopathy and heart failure caused by a mutation in phospholamban. *Science*. 299:1410-1413.
- Haghighi K, et al. 2003. Human phospholamban null results in lethal dilated cardiomyopathy revealing a critical difference between mouse and human. *J Clin Invest*. 111:869-876. doi:10.1172/JCI200317892.
- Xiao X, Li J, and Samulski RJ. 1998. Production of high-titer recombinant adeno-associated virus vectors in the absence of helper adenovirus. *J Virol*. 72:2224-2232.
- Auricchio A, Hinderling M, O'Connor E, Gao GP, and Wilson JM. 2001. Isolation of highly infectious and pure adeno-associated virus type 2 vectors with a single-step gravity-flow column. *Hum Gene Ther*. 12:71-76.
- Hongo M, et al. 1998. Angiotensin II blockade followed by growth hormone as adjunctive therapy after experimental myocardial infarction. *J Card Fail*. 4:213-224.
- Ryke T, et al. 1999. Progressive cardiac dysfunction and fibrosis in the cardiomyopathic hamster and effects of growth hormone and angiotensin-converting enzyme inhibition. *Circulation*. 100:1734-1743.
- Schiller NB, et al. 1989. Recommendations for quantitation of the left ventricle by two-dimensional echocardiography. American Society of Echocardiography Committee on Standards, Subcommittee on Quantitation of Two-Dimensional Echocardiograms. *J Am Soc Echocardiogr*. 2:358-367.
- Collins KA, Korcarz CE, and Lang RM. 2003. Use of echocardiography for the phenotypic assessment of genetically altered mice. *Physiol Genom*. 13:227-239.
- Sheehan FH, et al. 1986. Advantages and applications of the centerline method for characterizing regional ventricular function. *Circulation*. 74:293-305.
- Levin SE, Katz SE, Morgan JP, and Douglas PS. 1994. Serial echocardiographic assessment of left ventricular geometry and function after large myocardial infarction in the rat. *Circulation*. 89:345-354.
- Balak P, et al. 1997. Endothelial gaps: time course of formation and closure in inflamed venules of rats. *Am J Physiol*. 272:L155-L170.
- Tanaka M, et al. 1986. Quantitative analysis of myocardial fibrosis in normals, hypertensive hearts, and hypertrophic cardiomyopathy. *Br Heart J*. 55:575-581.
- Inada T, et al. 1999. Upregulated expression of cardiac endothelin-1 participates in myocardial cell growth in the B14.6 Syrian cardiomyopathic hamsters. *J Am Coll Cardiol*. 33:565-571.
- Frank K, Tilgmann C, Shannon RT, Bers DM, and Kranias EG. 2000. Regulatory role of phospholamban in the efficiency of cardiac sarcoplasmic reticulum Ca<sup>2+</sup> transport. *Biochemistry*. 39:14176-14182.
- Zhou YY, et al. 2000. Culture and adrenalectomy of adult mouse cardiac myocytes: methods for cellular genetic physiology. *Am J Physiol Heart Circ Physiol*. 279:H429-H436.
- Hajjar RJ, Schmidt U, Kang JX, Matsui T, and Rosenzweig A. 1997. Adenoviral gene transfer of phospholamban in isolated rat cardiomyocytes. Rescue effects by concomitant gene transfer of sarcoplasmic reticulum (Ca<sup>2+</sup>)-ATPase. *Circ Res*. 81:145-153.
- Molkentin JD, and Dorn IG. 2001. Cycloplasmic signaling pathways that regulate cardiac hypertrophy. *Annu Rev Physiol*. 63:391-426.
- Freedy N, McKinney TA, and Olson EN. 2000. Dyeing cardiac signals involved in cardiac growth and function. *Nat Med*. 6:1221-1227.
- Ramirez MT, Zhao XL, Schulman H, and Brown JH. 1997. The nuclear delta1 isoform of Ca<sup>2+</sup>/calmodulin-dependent protein kinase II regulates atrial natriuretic factor gene expression in ventricular myocytes. *J Biol Chem*. 272:31203-31208.
- Molkentin JD, et al. 1998. A calcineurin-dependent transcriptional pathway for cardiac hypertrophy. *Cell*. 93:215-228.
- Leite WC. 1985. The left ventricular dp/dtmax-end-diastolic volume relation in closed-chest dogs. *Circ Res*. 56:808-815.
- Li J, et al. 2003. Efficient and long-term intracardiac gene transfer in dilated-sarcoplasmic-deficiency hamster by adeno-associated virus-2 vectors. *Gene Ther*. 10:1807-1813.
- Smytheshwar R. 1989. Molecular mechanisms of myocardial remodeling. *Physiol Rev*. 79:215-262.
- Hayashida W, Van Eyck C, Rousseau MF, and Pouleur H. 1993. Regional remodeling and nonuniform changes in diastolic function in patients with left ventricular dysfunction: modification by long-term enalapril treatment. The SOLVD Investigators.

- J. Am. Coll. Cardiol.* 22:1403-1410.
40. Zafeiridis, A., Jeevanandam, V., Houser, S.R., and Margulies, K.B. 1998. Regression of cellular hypertrophy after left ventricular assist device support. *Circulation*. 98:656-662.
  41. Mukherjee, R., et al. 2003. Myocardial infarct expansion and matrix metalloproteinase inhibition. *Circulation*. 107:618-625.
  42. Nadal-Ginard, B., Kajstura, J., Leri, A., and Anversa, P. 2003. Myocyte death, growth, and regeneration in cardiac hypertrophy and failure. *Circ. Res.* 92:139-150.
  43. Mani, K., and Kitsis, R.N. 2003. Myocyte apoptosis: programming ventricular remodeling. *J. Am. Coll. Cardiol.* 41:761-764.
  44. Ross, J., Jr. 1991. Myocardial perfusion-contraction matching. Implications for coronary heart disease and hibernation. *Circulation*. 83:1076-1083.
  45. Knoll, R., et al. 2002. The cardiac mechanical stretch sensor machinery involves a Z disc complex that is defective in a subset of human dilated cardiomyopathy. *Cell*. 111:943-955.
  46. Hongo, M., et al. 2000. Effects of growth hormone on cardiac dysfunction and gene expression in genetic murine dilated cardiomyopathy. *Basic Res. Cardiol.* 95:431-441.
  47. Sasaki, T., Inui, M., Kimura, Y., Kuzuya, T., and Tada, M. 1992. Molecular mechanism of regulation of  $Ca^{2+}$  pump ATPase by phospholamban in cardiac sarcoplasmic reticulum. Effects of synthetic phospholamban peptides on  $Ca^{2+}$  pump ATPase. *J. Biol. Chem.* 267:1674-1679.
  48. Brittan, A.G., and Kranias, E.G. 2000. Phospholamban and cardiac contractile function. *J. Mol. Cell. Cardiol.* 32:2131-2139.
  49. Hagemann, D., and Xiao, R.P. 2002. Dual site phospholamban phosphorylation and its physiological relevance in the heart. *Trends Cardiovasc. Med.* 12:51-56.
  50. DeSantiago, J., Maier, L.S., and Bers, D.M. 2002. Frequency-dependent acceleration of relaxation in the heart depends on  $CaMKII$ , but not phospholamban. *J. Mol. Cell. Cardiol.* 34:975-984.
  51. Miyamoto, M.L., et al. 2000. Adenoviral gene transfer of SERCA2a improves left-ventricular function in aortic-banded rats in transition to heart failure. *Proc. Natl. Acad. Sci. U. S. A.* 97:793-798.
  52. Elizerna, K., et al. 2000. Adenovirus-based phospholamban antisense expression as a novel approach to improve cardiac contractile dysfunction: comparison of a constitutive viral versus an endothelin-1-responsive cardiac promoter. *Circulation*. 101:2193-2199.
  53. He, H., et al. 1999. Effects of mutant and antisense RNA of phospholamban on SR  $Ca^{2+}$ -ATPase activity and cardiac myocyte contractility. *Circulation*. 100:974-980.
  54. del Monte, F., Harding, S.E., Dec, G.W., Gwathmey, J.K., and Hajjar, R.J. 2002. Targeting phospholamban by gene transfer in human heart failure. *Circulation*. 105:904-907.
  55. Dierckx, T., et al. 2003. Gene transfer of contractilin, a recombinant inotropic antibody-based protein, improves cardiac function in the BIO 14.6 hamster. *J. Am. Coll. Cardiol.* 41(Suppl. A):217A. (Abstr.)
  56. Ikeda, Y., et al. 2000. Altered membrane proteins and permeability correlate with cardiac dysfunction in cardiomyopathic hamsters. *Am. J. Physiol. Heart Circ. Physiol.* 278:H1362-H1370.
  57. Ross, J., Jr. 1998. Adrenergic regulation of the force-frequency effect. *Basic Res. Cardiol.* 93:95-101.
  58. Smith-Adina, J.R., and Bartlett, J.S. 2001. Gene therapy: recombinant adeno-associated virus vectors. *Curr. Cardiol. Rep.* 3:43-49.
  59. Melo, L.G., et al. 2002. Gene therapy strategy for long-term myocardial protection using adeno-associated virus-mediated delivery of heme oxygenase gene. *Circulation*. 105:602-607.
  60. Brockstedt, D.G., et al. 1999. Induction of immunity to antigens expressed by recombinant adeno-associated virus depends on the route of administration. *Clin. Immunol.* 92:67-75.
  61. Stevenson, L.W. 1998. Inotropic therapy for heart failure. *N. Engl. J. Med.* 339:1848-1850.
  62. Marks, A.R., Prieo, S., Memmi, M., Kontula, K., and Laitinen, P.J. 2002. Involvement of the cardiac ryanodine receptor/calcium release channel in catecholaminergic polymorphic ventricular tachycardia. *J. Cell. Physiol.* 190:1-6.
  63. Picard, M.H., Wilkins, G.T., Ray, P.A., and Weyman, A.E. 1990. Natural history of left ventricular size and function after acute myocardial infarction. Assessment and prediction by echocardiographic endocardial surface mapping. *Circulation*. 82:484-494.



# Reversal of Calcium Cycling Defects in Advanced Heart Failure

## Toward Molecular Therapy

Masahiko Hoshijima, MD, PhD,\*† Ralph Knöll, MD, PhD,\* Mohammad Pashmforoush, MD, PhD,\*  
Kenneth R. Chien, MD, PhD,\*‡

La Jolla, California; and Boston, Massachusetts

Heart failure is a growing major cause of human morbidity and mortality worldwide. A wave of new insights from diverse laboratories has begun to uncover new therapeutic strategies that affect the molecular pathways within cardiomyocytes that drive heart failure progression. Using an integrative approach that employs insights from genetic-based studies in mouse and humans and in vivo somatic gene transfer studies, we have uncovered a new link between stress signals mediated by mechanical stretch and defects in sarcoplasmic reticulum (SR) calcium cycling. An intrinsic mechanical stress sensing system is embedded in the Z disc of cardiomyocytes, and defects in stretch responses can lead to heart failure progression and associated increases in wall stress. Reversal of the chronic increases in wall stress by promoting SR calcium cycling can prevent and partially reverse heart failure progression in multiple genetic and acquired model systems of heart failure in both small and large animals. We propose that reversal of advanced heart failure is possible by targeting the defects in SR calcium cycling, which may be a final common pathway for the progression of many forms of heart failure. (J Am Coll Cardiol 2006;48:A15-23) © 2006 by the American College of Cardiology Foundation

For heart failure patients and their physicians, these are the best of times and the worst of times. Over the past 3 decades, there have been major advances in the treatment of heart failure, ranging from an extensive list of medical therapy (beta-blockers, angiotensin-converting enzyme inhibitors, and so on), improvements in heart transplantation with new agents to suppress tissue rejection, and novel device technology (synchronized pacing/left ventricular assist devices, and so on). At the same time, despite these substantial clinical advances, heart failure has become the major cause of human cardiovascular morbidity and mortality worldwide, and has been predicted to reach epidemic proportions in the early period of the 21st century. The reasons for this clinical conundrum are undoubtedly multifactorial, reflecting the increasing lifespan, globalization of calorie-rich eating habits, the higher incidence of metabolic diseases and associated risk for ischemic heart disease, and the substantial improvement of the survival rate of acute coronary events. In fact, an exponential increase in the incidence of heart failure in China and India, followed by many other countries, is signaling an emerging global health problem of unprecedented proportions (1,2). At the core of this epidemic is our fundamental lack of understanding of the precise molecular pathways that drive human heart

failure (i.e., mechanisms underlying the progressive dilation of the cardiac chamber and the associated decreases in cardiac contractility). However, several laboratories have successfully utilized an integrative approach to dissect pathways that lead to dilated cardiomyopathy (DCM), employing genetic-based studies in mice and humans, in vivo somatic gene transfer, bioinformatics, advanced imaging technologies, and computational biology, which is beginning to provide new insights into the disease process, and suggesting new therapeutic targets and strategies for intervening in the disease (3-7). Accordingly, a growing body of evidence suggests that a major component of this process now appears to be chronic increases in wall stress that trigger specific stress-related signaling pathways for critical cell responses, which include cell death pathways, survival cues, hypertrophic responses, and associated changes in the downstream pathways (8,9). In this review, we describe recent advances that have led to the discovery of a pivotal role of defects in calcium cycling in the pathogenesis of human heart failure and the background that has led to a novel therapeutic strategy for reversal of these defects that will be slated for clinical studies in the coming year.

## CHARACTERIZATION OF A GENETICALLY BASED MODEL OF DCM AND HEART FAILURE IN MUSCLE-SPECIFIC LIM PROTEIN (MLP)-DEFICIENT MICE

One of the first genetic links between cardiac cytoskeletal defects and DCM was made via studies of mutant mice that harbor a deficiency in MLP (10). Muscle-specific LIM protein, also known as cysteine-rich protein 3 or cysteine- and glycine-rich protein 3 (CSR3P), is a member of the

From the \*Institute of Molecular Medicine and †Center for Research in Biological Systems, University of California San Diego, La Jolla, California; and the ‡Cardiovascular Research Center, Massachusetts General Hospital, Department of Cell Biology, Harvard Medical School, the Harvard Stem Cell Institute, Boston, Massachusetts. Supported by the Jean Leducq Foundation and an AHA National Scientist Development Award and NIH/NHLBI (HL081401) to Dr. Hoshijima. Jeffrey A. Towbin, MD, served as guest editor for this article.

Manuscript received February 7, 2006; revised manuscript received May 22, 2006, accepted June 22, 2006.

# Abbreviations and Acronyms

BNP	= brain natriuretic peptide
CM	= cardiomyopathy
CSR3	= cysteine- and glycine-rich protein 3
DCM	= dilated cardiomyopathy
HCM	= hypertrophic cardiomyopathy
MLP	= muscle-specific LIM protein
PKA	= protein kinase A
PLN	= phospholamban
post-MI	= post-myocardial infarction
rAAV	= recombinant adeno-associated virus
RyR	= ryanodine receptor
SERCA2	= sarcoplasmic reticulum calcium ATPase 2
SR	= sarcoplasmic reticulum
T-cap	= titin-cap
TTN	= titin

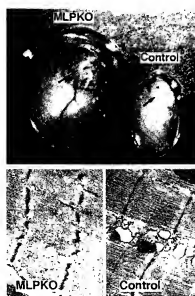
C-reactive protein gene family (11) and contains 2 highly conserved LIM domains that have been shown to serve as protein-protein interaction modules in a series of LIM proteins (12). Muscle-specific LIM protein is expressed in cardiac and skeletal muscle (10,13) and is predominantly localized in the cardiac cytoskeleton, mainly adjacent to the Z disc structure (10,14). Mutant mice with the genetic ablation of MLP display a cardiac phenotype that closely resembles human DCM, including progressive enlargement of all 4 cardiac chambers, ventricular wall thinning, decreases in cardiac contractility (10,15), induction of embryonic gene markers, defects in sarcoplasmic reticulum (SR)  $Ca^{2+}$  handling (15,16), with the elongation of action potential duration and the desensitization of beta-adrenergic signaling (10,17) (Fig. 1). In addition, genetic defects of CSR3/MLP (18–20) and abnormal CSR3/MLP expression (21) have been linked to cardiomyopathy and heart failure in

human patients. Thus, the MLP-null mouse serves as an ideal tool for unraveling pathways that lead to heart failure initiation and progression, as well as the identification of new therapeutic strategies via genetic complementation.

## AN MLP/TTIN-CAP (T-CAP)/Z DISC TTIN COMPLEX CONSTITUTES AN ESSENTIAL COMPONENT OF THE INTRINSIC MECHANICAL STRESS SENSOR MACHINERY IN CARDIOMYOCYTES

Utilizing the MLP-null mouse model of cardiomyopathy, we revealed a critical role for MLP as an essential component of the cardiac muscle stretch sensor (18). A combinatorial approach of yeast 2-hybrid screening of a cardiac cDNA library, glutathione S-transferase-pull down, and immuno-co-localization analyses identified a 19-kD cytoskeletal protein, T-cap (T-cap: telethonin), as a MLP-binding protein. This molecule localizes at the sarcomere Z disc and binds to the NH<sub>2</sub>-terminal Z disc domain of the titin molecule (Fig. 2). The T-cap interacting domain of MLP was identified in a short NH<sub>2</sub>-terminal domain of MLP that precedes the first LIM domain (18). Immuno-staining of T-cap in the MLP-null myocardium demonstrated that T-cap was dissociated from Z disc and diffused out in the cytoplasm in a fraction of cardiomyocytes, indicating the possibility that MLP stabilizes T-cap interaction with the NH<sub>2</sub>-terminal Z disc-associated domain of titin. In addition, electric-microscopic examination of MLP-null myocardium demonstrated that the MLP-null Z disc was widened, brushed, and wavy compared with wild-type control animals.

Titin serves a structural role in cardiac muscle in sarcomeric organization and assembly, as well as playing a crucial role in restoring cardiac sarcomeric length and in aligning the M-band at the center of the sarcomere during each

		MLPKO	human DCM
	Ventricular dilatation	+	+
	Ventricular wall thickness	thin	thin
	Atrial dilatation	+	+
	Interstitial fibrosis	+	+
	Cardiomyocyte dropout	+	+
	Myocyte hypertrophy	+	+
	Myofilament disarray	+	+
	Z disc thickening	+	?
	Ventricular contractility	low	low
	Cardiac output	low	low
	Ventricular relaxation	impaired	impaired
	$\beta$ AR responses	desensitized	desensitized
	SR calcium cycling	impaired	impaired
	Ventricular APD	prolonged	prolonged
Embryonic gene program		+	+

**Figure 1.** Muscle-specific LIM protein (MLP)-deficient (MLPKO) mice share a broad spectrum of pathological phenotypes with human dilated cardiomyopathy (DCM). Note defective Z disc found in the MLP-null myocardium. APD = action potential duration; SR = sarcoplasmic reticulum;  $\beta$ AR = beta-adrenergic receptor.

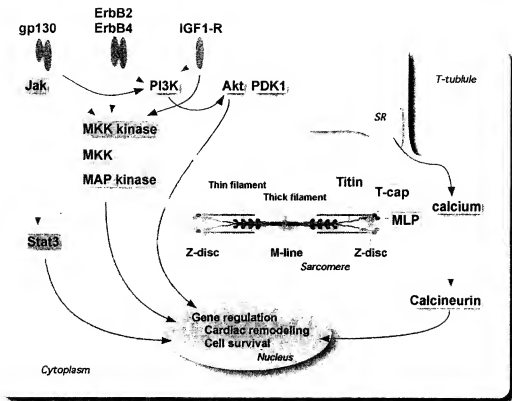


**Figure 2.** Z disc-related mechanical sensor cross-talks with receptor-dependent signaling. Transmembrane receptors including gp130 cytokine receptors, erbB2-erbB4, and insulin-like growth factor-1 receptor (IGF1-R) activate multiple signal kinase cascades that regulate cell protective gene programs. A calcium-activated calcineurin dephosphorylates multiple cellular substrates including transcriptional regulators that regulate cardiac remodeling. Cardiomyocytes, on the other hand, have (perhaps multiple) mechanical stress sensors inside of the cells, and the titin-T-cap-muscle-specific LIM protein (MLP) complex constitutes such a sensor systems associated with Z discs (24). Akt = protein kinase B; Jak = Janus kinase; MAP = mean arterial pressure; MKK = mitogen-activated protein kinase kinase; PDK1 = phosphoinositide-dependent protein kinase 1; SR = sarcoplasmic reticulum; Stat3 = signal transducer and activator of transcription-3.

cardiac contraction (22,23). Titin is anchored at the Z disc with its NH<sub>2</sub>-terminal strongly associated with the actin thin filament that is cross-linked by  $\alpha$ -actinin. Interestingly, in vitro physiological measurements revealed that MLP-null cardiac papillary muscles from 2-week-old MLP-null mice (before the development of general cardiac dysfunction), displayed a selective defect in the mechanical stretch properties of titin, with impairment in tension generation starting at a short range (within 10%) of passive stretch (18). Furthermore, cultured MLP-deficient neonatal day 1 to 3 cardiac muscle cells displayed a nearly complete loss of passive stretch-dependent induction of a genetic marker of cardiac mechanical stress, brain natriuretic peptide (BNP) (18). Importantly, the same MLP-null cardiomyocytes retained a normal BNP induction in response to G-protein coupling membrane receptor stimulation, providing direct support for a selective defect in mechanical stress sensing functions in MLP-null cardiac muscle. Taken together, our studies in MLP-null cardiomyocytes revealed that an MLP interaction with T-cap at the Z disc is critical to maintain the mechanical elastic properties of titin and that MLP/T-cap/Z disc-titin complex constitutes a critical molecular component of the cardiac muscle stretch sensor (24). In this manner, a loss or dysfunction of this intrinsic mechanical stress sensing machin-

ery linked to the Z disc-titin structure may lead to the development of heart failure and DCM via the loss of the ability to activate stretch-mediated survival cues. Such survival cues could occur via the gp130-dependent, neuregulin-ErbB2/erbB4-induced, or insulin-like growth factor-1-activated cardiomyocyte survival pathway (25-29) (Fig. 2), or calcineurin-dependent pro-hypertrophic nuclear gene regulatory pathway (30).

#### CSR3P/MLP MUTATIONS ASSOCIATED WITH FAMILIAL DILATED AND HYPERTROPHIC CARDIOMYOPATHIES (HCMS)

Since the discovery of the MLP mouse model of DCM, a growing list of genetic defects have been found in cytoskeletal proteins (7,31), as well as in extracellular matrix proteins that serve an anchoring function with the sarcolemmal cytoskeletal complex (32), linking them to the familial forms of cardiomyopathies. CSR3P (human MLP) is encoded by an approximately 20-kb genomic sequence with 6 exons. We started with sequencing the CSR3P coding exons of genomic DNAs obtained from selected DCM patients, followed by polymerase chain reaction-based selective single nucleotide change analyses for 536 well-phenotyped

Caucasian patients bearing familial DCM together with 320 control individuals with the same demographic distribution. Consequently, we identified a close association between 10 of 536 human DCM patients and a sense nucleotide alteration of CSR3P (i.e., CSR3P[W4R]) in a highly conserved amino acid residue within the N-terminal T-cap binding domain (18). The linkage analysis in these families is limited by several factors, including the size of available pedigrees and age-dependent penetrance. Interestingly, the haplotype analysis supported a founder effect in a DCM patient population with CSR3P(W4R), although there were no linking records of affinity between patient families.

After the publication of our original report, at least 3 studies have analyzed CSR3P(W4R) in DCM and HCM patients. One study found CSR3P(W4R) in a family with DCM; however, CSR3P(W4R) did not segregate with DCM in this family (20). In another study, CSR3P(W4R) was found in 7 of 389 unrelated HCM patients with 1 in 400 reference alleles, and, interestingly, 3 HCM patients with CSR3P(W4R) also carried mutations of either beta-myosin heavy chain or myosin binding protein-C (33). Finally, a Canadian study reported 1 HCM patient with CSR3P(W4R) of 192, whereas CSR3P(W4R) was also found in 3 of 250 control individuals, who are predominantly of British Isles origin and did not receive formal cardiologic examination (34). Accordingly, it is plausible that CSR3P(W4R) is a genetic modifier or a relatively rare polymorphism that segregates with a subset of the cardiomyopathy population, rather than a disease-causing variant. Besides the W4R variant, other nucleotide changes (L44P, S54R/E55G, C58G, K69R) in the CSR3P gene have recently been reported in patients with cardiomyopathies (19,20). The amino acid positions of these additional mutations are outside of the T-cap interacting domain of CSR3P.

Although genetic evidence is somewhat obscure, there was a strong biological finding to support the role of the CSR3P(W4R) amino acid substitution in the pathogenesis of DCM. The CSR3P(W4R) resulted in the complete loss of T-cap interaction shown by the yeast 2-hybrid analysis, and myocardial biopsies from a DCM patient harboring a CSR3P(W4R) allele showed partial T-cap dissociation from the Z disc. The biological significance of MLP/T-cap interaction in the maintenance of normal cardiac function was further emphasized by our independent identification of a single proband with the R87Q mutation of TCAP (human T-cap gene) in a set of Caucasian DCM patients (18). The R87 amino acid residue was mapped within the MLP-interacting domain of T-cap, and TCAP(R87Q) mutant protein displayed a ~80% reduction in binding affinity to MLP (35). Interestingly, other mutations in TCAP are linked to Limb-Girdle Muscular Dystrophy type 2G (36), suggesting that T-cap interaction with the Z disc-titin structure is requisite to maintain physiological functions of both cardiac and skeletal muscle. Herein, human titin (TTN) mutations have been linked to familial DCM (37,38), and a mutation was also found in an HCM patient (39). As a recent study proposes a model of N-terminal titin assembly that is mediated by the

dimerization of T-cap in an antiparallel manner (40), we speculate that mutations of CSR3P, TCAP, and TTN share a common molecular pathway to induce and/or modulate the development of cardiomyopathy.

## IDENTIFICATION OF SR CALCIUM CYCLING AS A MAJOR TARGET TO TREAT DCM AND HEART FAILURE: PHOSPHOLAMBAN (PLN) ABLATION RESCUES HEART FAILURE IN THE SUBSETS OF MOUSE MODELS OF DCM

Defects in SR  $\text{Ca}^{2+}$  cycling are a highly conserved signature feature of experimental and human heart failure. The most notable abnormalities are a decrease in the  $\text{Ca}^{2+}$  re-entry mechanism into the SR, which is predominantly governed by the activity of the SR calcium ATPase 2 (SERCA2) and dysregulated  $\text{Ca}^{2+}$  release from SR through ryanodine receptor (RyR) (Fig. 3A). In both cases, the SR calcium level is largely diminished in failing hearts, creating defects in both diastolic and systolic functions. In this manner, a decrease in the quantal release of calcium from SR through RyR during systole affects the contractility of individual cardiomyocytes, whereas the impaired calcium pump function results in a defect in ventricular relaxation. Cardiac muscle cells have an endogenous inhibitor of SERCA2, namely PLN, which is a highly conserved 52-amino-acid peptide and the expression of which is largely restricted in the heart and slow skeletal muscle. Phospholamban is phosphorylated by the cyclic adenosine monophosphate (AMP)-dependent protein kinase (PKA) that is regulated by G-protein coupling receptors including  $\beta$ -adrenergic receptors, and this phosphorylation in turn releases the PLN inhibitory effects on the SERCA2 activity (41,42). In many forms of human and experimental heart failure, the down-regulation of the SERCA2 expression level, impairments in the SERCA2/PLN ratio, and a decrease in the phosphorylated form of PLN have been documented (42–44). Whether these changes are part of abnormal cardiac remodeling in the development of heart failure or represent an adaptive process to limit cardiac function and reduce cardiac energy consumption to protect cardiomyocytes has been a point of discussion. To address this question, we utilized a genetic complementation strategy, which ultimately provided strong evidence that defects in SR  $\text{Ca}^{2+}$  cycling play a pivotal role in heart failure progression. We generated double knockout mice, which harbor the MLP-null cardiomyopathic mutation, but also lack PLN, and subsequently examined whether removing PLN inhibition alone would have a measurable effect on heart failure progression. Remarkably, the ablation of PLN completely prevented the spectrum of heart failure phenotypes found in a mouse model of DCM caused by MLP deficiency (16).

Subsequent studies designed to test PLN ablation in various forms of cardiomyopathy and heart failure reported mixed results (45–47). In some forms of transgenic cardiomyopathy mouse models, PLN-null rescued cardiomyopa-

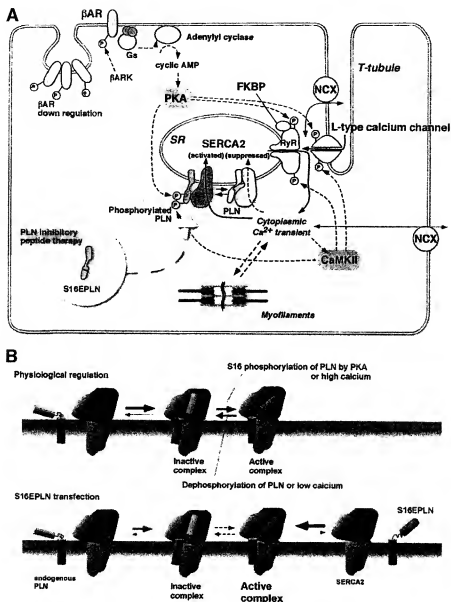


**Figure 3.** Regulatory systems of cardiac excitation-contraction coupling and the gene therapy targeting sarcoplasmic reticulum (SR) calcium uptake. (A) Intracellular mobilization of calcium ions governs myofilament contraction and relaxation. Two calcium release channels, the L-type calcium channel and ryanodine receptor (RyR), and a regulator of SR calcium uptake, phospholamban (PLN), are key controllers of calcium mobilization under the control of 2 second-messenger-regulated kinases, cyclic adenosine monophosphate (AMP)-dependent kinase (PKA) and calcium-calmodulin-dependent kinase II (CaMKII) (42). 51E6PLN therapy directly targets SR calcium uptake (see text for details). (B) A working model of PLN-dependent SR calcium ATPase 2 (SERCA2) regulation has been refined, based on recent studies by Mueller et al. (61) and Zamoon et al. (62). Phospholamban is tightly bound to SERCA2 due to their low dissociation constant. Physiologically, high calcium concentration or PLN phosphorylation induces conformational changes of the cytoplasmic domain of PLN, which results in a structural rearrangement of the PLN-SERCA2 interaction (from an inactive complex to an active complex) with subsequent increase in SERCA2 activity and calcium uptake. The gene therapy for PLN-2A2 interaction can greatly contribute to an active PLN-SERCA2 complex in cardiomyocytes. ARK = adrenergic receptor kinase;  $\beta$ AR =  $\beta$ -adrenergic receptor; FKBP = K506 binding protein; NCX = Na-Ca exchanger.

thy phenotypes, while benefits were unclear in other model systems. Obviously there are limitations to the use of genetically based models to validate new therapeutic strategies for acquired forms of human heart failure. Indeed, most of these models have not been validated with respect to their fidelity of predicting therapeutic efficacy in the clinical setting. Furthermore, it would be pivotal to evaluate the effects of the reversal of the calcium cycling defect on heart

failure after it had already been fully established as opposed to examining effects to prevent the initial onset. In this regard, as described in subsequent sections, we tested the PLN inhibitory therapy in 2 well-established and fully validated small animal heart failure models; one is a genetic form and the other is surgically induced, both of which have a long history of extensive use for a wide variety of pharmacological therapy. In both cases, PLN inhibition was

induced by cardiac-targeted somatic gene transfer (Fig. 3A), substantially after the onset of heart failure and during its disease progression, to allow a direct examination as to whether improvement of calcium cycling defects might lead to a reversal of components of the heart failure phenotype.

## PLN INHIBITION RESCUES HEART FAILURE IN THE HAMSTER MODEL OF LIMB-GIRDLE MUSCULAR DYSTROPHY AND CARDIOMYOPATHY

To allow long-term, high efficiency, in-vivo transcortical delivery and expression of foreign genes, we first developed a new transcortical gene delivery system that utilized a recombinant adeno-associated virus (AAV) vector (48). The therapeutic payload of the vector was a PLN inhibitory peptide, which consisted of a pseudo-phosphorylated mutant of PLN with a single amino-acid change at the position Ser16 to Glu (S16EPLN), designed to mimic the conformational change in PLN after phosphorylation by PKA (Fig. 3B). This S16EPLN/ $\tau$ AAV vector was then used to constitutively activate SR  $\text{Ca}^{2+}$  cycling in the myocardium of the well-characterized small animal model of chronic heart failure and DCM, the BIO14.6 cardiomyopathic (CM) hamster, which is based on a mutation in the  $\delta$ -sarcoglycan gene. This genetic defect represents an autosomal recessive form of human myopathy found in limb-girdle muscular dystrophy type F (49). Although cardiac involvement of human limb-girdle muscular dystrophy is generally mild,  $\delta$ -sarcoglycan deficiency in small animals including the BIO14.6 CM hamster and its derivatives and  $\delta$ -sarcoglycan knockout mice causes an aggressive form of cardiomyopathy (50,51). Although there is an ongoing debate whether sarcolemmal defects in cardiomyocytes are a primary cause of  $\delta$ -sarcoglycan-null cardiomyopathy or vascular abnormality contributes to its pathogenesis (52–54), sarcolemmal fragility may be a common pathological process of cardiomyopathies that are induced by genetic defects of cortical cytoskeletal proteins (52,53) or their secondary defects (55). Interstitial and replacement fibrosis also contributes to the pathological process of cardiomyopathy in BIO14.6 CM hamsters (52,53).

Nevertheless, the chronic inhibition of PLN by the S16EPLN peptide resulted in a marked enhancement of cardiac diastolic and systolic function even at advanced stages of the disease over 7 months from the initial delivery of the gene (48). Accordingly, the S16EPLN was capable of inducing the stable activation of SERCA2 and resulted in the enhancement of cardiac relaxation and subsequent contractility in the absence of adrenergic stimuli, which was analogous to the null phenotype of the PLN mutant mice (16).

## PLN INHIBITION RESCUES HEART FAILURE DEVELOPMENT IN THE RAT MODEL OF POST-MYOCARDIAL INFARCTION (POST-MI) CHRONIC HEART FAILURE

The rAAV-mediated pseudo-phosphorylated PLN gene transfer therapy was tested in the chronic failing hearts of

post-MI rats (56). Pre-gene transfer echocardiography documented that the recipient mouse (5 weeks after myocardial infarction surgery, with 30% to ~40% infarction size selected by echocardiography) had a moderate level of heart failure with the average percent fractional shortening as 32.4%, compared with the sham control animals (average percent fractional shortening, 53.1%). Eighty-five percent animals survived the gene transfer procedure, which was mostly similar to that used for the preceding BIO14.6 CM hamster studies, and the therapeutic prognosis was evaluated by repeated echocardiography over 6 months (Figs. 4A to 4F).

The left ventricular ejection fraction was enhanced by 6.0% at 2 months compared with the pre-gene transfer baseline value and by 12.8% at 6 months in S16EPLN-treated MI-rats, in contrast with the progressive decline of left ventricular ejection fraction in saline-treated control post-MI animals (Fig. 4C). Change in the left ventricular end-diastolic volume of S16EPLN-treated rat from the pre-gene transfer to the end point was limited to 18.2%, which was indistinguishable with sham rats and was considered proportional to the natural growth of animals (Fig. 4A), suggesting the complete suppression of progressive left ventricular dilation by the S16EPLN therapy in post-MI rats (note the left ventricles of saline-treated control post-MI animals continued to enlarge, as shown in Fig. 4A). Hemodynamic analyses further confirmed the improvement of left ventricular function by the S16EPLN/ $\tau$ AAV strategy (56). Among other improvements, the left ventricular end-diastolic pressure, which was considerably elevated in MI-saline rats, was near normal in the S16EPLN treatment group (56). In quantitative histologic analysis, a significantly lower extent of interstitial fibrosis (Fig. 4I) and suppression of cardiomyocyte hypertrophy were apparent in the non-infarct region in the S16EPLN-treated animals versus the control group (56). Taken together, these results indicate that enhancing calcium cycling by inhibiting PLN was capable of significantly enhancing multiple independent parameters of cardiac function even in the setting of the loss of over 30% of the viable myocardium.

## CLINICAL APPLICATION OF PLN INHIBITION THERAPY AND OTHER THERAPIES TO ENHANCE SR $\text{Ca}^{2+}$ UPTAKE

Previous clinical studies questioned the relevancy of the use of inotropic agents to treat chronic heart failure. There was evidence that chronic exposure to positive inotropic agents, such as catecholamines or phosphodiesterase inhibitors, can lead to a long-term decrease in cardiac function and an associated decrease in survival (57). Furthermore, administration of beta-blockers is now a mainstream heart failure treatment together with the afterload reduction therapy with angiotensin-converting enzyme inhibitors, improving survival and the progression of clinical heart failure (58). As noted in the current review, we consider defects in calcium

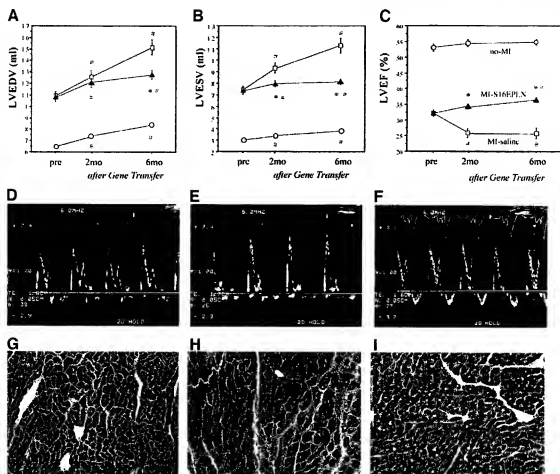


**Figure 4.** Chronic therapeutic effects of S16EPLN/rAAV-treatment in post-myocardial infarction (MI) rats. Serial changes of echocardiographic variables (A to C) before and after S16EPLN gene transfer and pulse-wave Doppler imaging of mitral flow found in sham (no-MI) rats (D), saline-treated post-MI rats (E), and S16EPLN-treated post-MI rats (F). Note elevated early filling velocity and diminished late filling found in saline-treated post-MI rats were normalized in S16EPLN-treated animals. Suppression of the induction of interstitial fibrosis in the non-infarcted region in S16EPLN-treated animals was obvious (G to I). (G) Sham (no-MI) rat myocardium; (H) Saline-treated post-MI rat myocardium; (I) S16EPLN-treated post-MI rat myocardium. Modified from figures in Iwanaga et al. (56). LVEDV = left ventricular end-diastolic volume; LVEF = left ventricular ejection fraction; LVESV = left ventricular end-systolic volume.

cycling are a final common pathway for decreases in cardiac function in advanced forms of the disease, irrespective of the etiology. The unique aspect of S16EPLN/rAAV gene therapy, in contrast with the preceding pharmacologic inotropic agents, is that this therapy targets the most downstream point of the regulatory pathway of excitation-contraction coupling without chronic increases in cytoplasmic cyclic AMP levels or chronic PKA activation. Accordingly, chronic improvement of excitation-contraction coupling in a cyclic AMP-independent manner with a high efficiency, long-term, and cardiotropic S16EPLN/rAAV gene delivery appear to be a novel therapeutic strategy for slowing heart failure progression. The inherent cardiac and slow skeletal muscle specificity determined by the native distribution of PLN is another safety aspect of S16EPLN therapy for clinical applications. It should be also noted that a large body of independent work by del Monte and Hajjar (59) elegantly moved forward to work on the potential therapeutic role of SERCA2 gene therapy for advanced forms of

heart failure, suggesting another approach to target defects in SR calcium cycling in heart failure.

To translate the SR calcium-targeted therapy to human clinical settings, we have been collaborating with Drs. David Kaye and John Powers of Baker Heart Institute in Melbourne, Australia, on the development of a novel clinically relevant, percutaneous gene delivery system with viral vectors (60). A unique strategy of safe, reproducible, high-efficient delivery of rAAV vectors (serotype 1 and serotype 2) to the myocardium of both healthy normal sheep and sheep with moderate-to-severe pacing-induced heart failure has been proven to be very reproducible. The catheter-based intracoronary SERCA2 or S16EPLN delivery involves recirculation of vectors in a closed-loop system, and this strategy has been shown to enhance cardiac contractility in heart failure in sheep.

These studies have set the stage for AAV gene therapy to enhance calcium cycling as a new therapeutic strategy for human heart failure, and the design of clinical studies is

moving forward in the near future. At the same time, the potential for developing small molecule inhibitors of PLN also needs to be reconsidered, given recent evidence that PLN actually represents an inhibitory subunit of SERCA (Fig. 3B), supported by recent elegant studies of Mueller et al. (61) and Zamoon et al. (62). Thus, the potential for the development of allosteric inhibitors of PLN remains a real possibility. New molecular-based strategies for enhancing calcium cycling appear to be on the horizon and may offer new hope for patients with advanced forms of the disease in the future.

## Acknowledgment

The authors thank the Jean Leducq Foundation for supporting these studies.

**Reprint requests and correspondence:** Dr. Kenneth R. Chien, Massachusetts General Hospital, Cardiovascular Research Center, Richard B Simches Research Center, CPZN 3208, 185 Cambridge Street, Boston, Massachusetts 02144-2790. E-mail: kchien@partners.org.

## REFERENCES

- Sanderson JE, Tse TF. Heart failure: a global disease requiring a global response. *Heart* 2003;89:585-6.
- Yusuf S, Vaz M, Pais P. Tackling the challenge of cardiovascular disease burden in developing countries. *Am Heart J* 2004;148:1-4.
- Hoshijima M, Chien KR. Mixed signals in heart failure: cancer rules. *J Clin Invest* 2002;109:849-55.
- Olson EN. A decade of discoveries in cardiac biology. *Nat Med* 2004;10:467-74.
- Robbins J. Genetic modification of the heart: exploring necessity and sufficiency in the past 10 years. *J Mol Cell Cardiol* 2004;36:643-52.
- Ahmad F, Seidman JG, Seidman CE. The genetic basis for cardiac remodeling. *Annu Rev Genomics Hum Genet* 2005;6:185-216.
- Towbin JA, Bowles NE. The failing heart. *Nature* 2002;415:227-33.
- Hunter JJ, Chien KR. Signaling pathways for cardiac hypertrophy and failure. *N Engl J Med* 1999;341:1276-83.
- Chien KR. Stress pathways and heart failure. *Cell* 1999;98:555-8.
- Arber S, Hunter JJ, Ross J Jr., et al. MLP-deficient mice exhibit a disruption of cardiac cytoarchitectural organization, dilated cardiomyopathy, and heart failure. *Cell* 1997;88:393-403.
- Weiskirchen R, Pino JD, Macalata T, Bister K, Beckerle MC. The cysteine-rich protein family of highly related LIM domain proteins. *J Biol Chem* 1995;270:28946-54.
- Bach I. The LIM domain: regulation by association. *Mech Dev* 2000;91:5-17.
- Arber S, Halder G, Caroni P. Muscle LIM protein, a novel essential regulator of myogenesis, promotes myogenic differentiation. *Cell* 1994;79:221-31.
- Henderson JR, Pomes P, Auffray C, Beckerle MC. ALP and MLP distribution during myofibrillogenesis in cultured cardiomyocytes. *Cell Motil Cytoskeleton* 2003;54:254-65.
- Esposito G, Santana LF, Dilly K, et al. Cellular and functional defects in a mouse model of heart failure. *Am J Physiol Heart Circ Physiol* 2000;279:H101-12.
- Minamitani S, Hoshijima M, Chu G, et al. Chronic phospholamban sarcoplasmic reticulum calcium ATPase interaction is the critical calcium cycling defect in dilated cardiomyopathy. *Cell* 1999;99:313-22.
- Rockman HA, Chien KR, Choi DJ, et al. Expression of a beta-adrenergic receptor kinase 1 inhibitor prevents the development of myocardial failure in gene-targeted mice. *Proc Natl Acad Sci U S A* 1998;95:7000-5.
- Knoll R, Hoshijima M, Hoffman HM, et al. The cardiac mechanical stretch sensor machinery involves a Z disc complex that is defective in a subset of human dilated cardiomyopathy. *Cell* 2002;111:943-55.
- Geier C, Perrot A, Ozcelik C, et al. Mutations in the human muscle LIM protein gene in families with hypertrophic cardiomyopathy. *Circulation* 2003;107:1390-5.
- Mohapatra B, Jimenez S, Lin JH, et al. Mutations in the muscle LIM protein and alpha-actinin-2 genes in dilated cardiomyopathy and endocardial fibroelastosis. *Mol Genet Metab* 2003;80:207-15.
- Zolk O, Caroni P, Bohm M. Decreased expression of the cardiac LIM domain protein MLP in chronic human heart failure. *Circulation* 2000;101:2674-7.
- Gregorio CC, Granzier H, Sorimachi H, Labeit S. Muscle assembly: a titanic achievement? *Curr Opin Cell Biol* 1999;11:18-25.
- Granzier H, Labeit D. Cardiac titin: an adjustable multi-functional spring. *J Physiol* 2002;541:335-42.
- Hoshijima M. Mechanical stress-strain sensors embedded in cardiac cytoskeleton: Z disc, titin, and associated structures. *Am J Physiol Heart Circ Physiol* 2006;290:H1313-25.
- Hirota H, Chen J, Betz UA, et al. Loss of a gp130 cardiac muscle cell survival pathway is a critical event in the onset of heart failure during biomechanical stress. *Cell* 1999;97:189-98.
- Yasukawa H, Hoshijima M, Gu Y, et al. Suppressor of cytokine signaling-3 is a biomechanical stress-inducible gene that suppresses gp130-mediated cardiac myocyte hypertrophy and survival pathways. *J Clin Invest* 2001;108:1459-67.
- Crone SA, Zhao YY, Fan L, et al. ErbB2 is essential in the prevention of dilated cardiomyopathy. *Nat Med* 2002;8:459-65.
- Garcia-Rivello H, Taranda J, Said M, et al. Dilated cardiomyopathy in ErbB4-deficient ventricular muscle. *Am J Physiol Heart Circ Physiol* 2005;289:H1153-60.
- Chien K. Heartpump and the heart—a molecular modifier of cardiac failure. *N Engl J Med* 2006;354:789-90.
- Frey N, Olson EN. Cardiac hypertrophy: the good, the bad, and the ugly. *Annu Rev Physiol* 2003;65:45-79.
- Morita H, Seidman J, Seidman CE. Genetic causes of human heart failure. *J Clin Invest* 2005;115:518-26.
- Wang J, Hoshijima M, Lam J, et al. Cardiomyopathy associated with microcirculatory dysfunction in laminin alpha4 chain-deficient mice. *J Biol Chem* 2006;281:213-20.
- Box JM, Poley RN, Ny M, et al. Genotype-phenotype relationships involving hypertrophic cardiomyopathy-associated mutations in titin, muscle LIM protein, and telethonin. *Mol Genet Metab* 2006;88:78-85.
- Newman B, Cescon D, Woo A, et al. W4R variant in CSRP3 encoding muscle LIM protein in a patient with hypertrophic cardiomyopathy. *Mol Genet Metab* 2005;84:374-5.
- Hayashi T, Arimura T, Itoh-Satoh M, et al. Tcap gene mutations in hypertrophic cardiomyopathy and dilated cardiomyopathy. *J Am Coll Cardiol* 2004;44:2192-201.
- Moreira ES, Wiltshire TJ, Faulkner G, et al. Limb-girdle muscular dystrophy type 2G is caused by mutations in the gene encoding the sarcomeric protein telethonin. *Nat Genet* 2000;24:163-6.
- Gerull B, Gramlich M, Atherton J, et al. Mutations of TTN, encoding the giant muscle filament titin, cause familial dilated cardiomyopathy. *Nat Genet* 2002;30:201-4.
- Siu BL, Nishimura H, Osborne JA, et al. Familial dilated cardiomyopathy locus maps to chromosome 2q31. *Circulation* 1999;99:1022-6.
- Sato M, Takahashi M, Sakamoto T, Hino M, Marumo F, Kimura A. Structural analysis of the titin gene in dilated cardiomyopathy: identification of a novel disease gene. *Biochem Biophys Res Commun* 1999;262:411-7.
- Zou P, Pinos N, Lange S, et al. Palindromic assembly of the giant muscle protein titin in the sarcomeric Z-disc. *Nature* 2006;439:229-33.
- Bers DM. Cardiac excitation-contraction coupling. *Nature* 2002;415:198-205.
- Hoshijima M. Gene therapy targeted at calcium handling as an approach to the treatment of heart failure. *Pharmacol Ther* 2005;105:211-28.
- Tomaselli GF, Marban E. Electrophysiological remodeling in hypertrophy and heart failure. *Cardiovasc Res* 1999;42:270-83.
- Hasenfuss G, Pieske B. Calcium cycling in congestive heart failure. *J Mol Cell Cardiol* 2002;34:951-69.
- Chien KR, Ross J Jr., Hoshijima M. Calcium and heart failure: the cycle game. *Nat Med* 2003;9:508-9.



46. Sobie EA, Guatimosim S, Song LS, Lederer WJ. The challenge of molecular medicine: complexity versus Occam's razor. *J Clin Invest* 2003;111:801-3.
47. Dorn GW 2nd, Molkentin JD. Manipulating cardiac contractility in heart failure: data from mice and men. *Circulation* 2004;109:150-8.
48. Hoshijima M, Ikeda Y, Iwanaga Y, et al. Chronic suppression of heart-failure progression by a pseudophosphorylated mutant of phospholamban via in vivo cardiac rAAV gene delivery. *Nat Med* 2002;8:864-71.
49. Straub V, Campbell KP. Muscular dystrophies and the dystrophin-glycoprotein complex. *Curr Opin Neurol* 1997;10:168-75.
50. Coral-Vazquez R, Cohn RD, Moore SA, et al. Disruption of the sarcoglycan-sarcospan complex in vascular smooth muscle: a novel mechanism for cardiomyopathy and muscular dystrophy. *Cell* 1999;98:465-74.
51. Hack AA, Lam MY, Cordier L, et al. Differential requirement for individual sarcoglycans and dystrophin in the assembly and function of the dystrophin-glycoprotein complex. *J Cell Sci* 2000;113:2535-44.
52. Durbeej M, Campbell KP. Muscular dystrophies involving the dystrophin-glycoprotein complex: an overview of current mouse models. *Curr Opin Genet Dev* 2002;12:349-61.
53. Wheeler MT, McNally EM. Sarcoglycans in vascular smooth and striated muscle. *Trends Cardiovasc Med* 2003;13:238-43.
54. Wheeler MT, Allikian MJ, Heydemann A, Hadhazy M, Zarnegar S, McNally EM. Smooth muscle cell-extrinsic vascular spasm arises from cardiomyocyte degeneration in sarcoglycan-deficient cardiomyopathy. *J Clin Invest* 2004;113:668-75.
55. Toyo-Oka T, Kawada T, Nakata J, et al. Translocation and cleavage of myocardial dystrophin as a common pathway to advanced heart failure: a scheme for the progression of cardiac dysfunction. *Proc Natl Acad Sci U S A* 2004;101:7381-5.
56. Iwanaga Y, Hoshijima M, Gu Y, et al. Chronic phospholamban inhibition prevents progressive cardiac dysfunction and pathological remodeling after infarction in rats. *J Clin Invest* 2004;113:727-36.
57. Stevenson LW. Inotropic therapy for heart failure. *N Engl J Med* 1998;339:1848-50.
58. Braunwald E. Expanding indications for beta-blockers in heart failure. *N Engl J Med* 2001;344:1711-2.
59. del Monte F, Hajjar RJ. Targeting calcium cycling proteins in heart failure through gene transfer. *J Physiol* 2003;546:49-61.
60. Kaye DMC, Chien KR, Hoshijima M, et al. Recirculating delivery of a pseudophosphorylated mutant of phospholamban or the sarcoplasmic reticulum Ca<sup>2+</sup> ATPase prevents the Progression of Heart Failure in a Large Animal Model (abstr). *Circulation* 2005;112:U68-9.
61. Mueller B, Karim CB, Negashov IV, Kutchai H, Thomas DD. Direct detection of phospholamban and sarcoplasmic reticulum Ca-ATPase interaction in membranes using fluorescence resonance energy transfer. *Biochemistry* 2004;43:8754-65.
62. Zamoon J, Nitu F, Karim C, Thomas DD, Veglia G. Mapping the interaction surface of a membrane protein: unveiling the conformational switch of phospholamban in calcium pump regulation. *Proc Natl Acad Sci U S A* 2005;102:4747-52.